

석사학위논문

Master's Thesis

네트워크 모델을 통한 전도도의 복구

Network approach to conductivity recovery

이민기 (李民基 Lee, Min-Gi)

수리과학과

Department of Mathematical Sciences

한국과학기술원

Korea Advanced Institute of Science and Technology

2009

네트워크 모델을 통한 전도도의 복구

Network approach to conductivity recovery

Network approach to conductivity recovery

Advisor : Professor Kim, Yong-Jung

by

Lee, Min-Gi

Department of Mathematical Sciences

Korea Advanced Institute of Science and Technology

A thesis submitted to the faculty of the Korea Advanced Institute of Science and Technology in partial fulfillment of the requirements for the degree of Master of Science in the Department of Mathematical Sciences

Daejeon, Korea

2009. 05. 26.

Approved by

Professor Kim, Yong-Jung

Advisor

네트워크 모델을 통한 전도도의 복구

이 민 기

위 논문은 한국과학기술원 석사학위논문으로 학위논문심사위원회에서 심사 통과하였음.

2009년 05월 26일

심사위원장 김 용 정 (인)

심사위원 이 창 옥 (인)

심사위원 김 홍 오 (인)

MMAS 이 민 기. Lee, Min-Gi. Network approach to conductivity recovery. 네트워크 모
20074181 델을 통한 전도도의 복구. Department of Mathematical Sciences . 2009. 43p.
Advisor Prof. Kim, Yong-Jung. Text in English.

Abstract

Inverse Problem on MREIT is a problem that finding electrical impedance of internal body by internal electrical relation governed by maxwell's equation. The simplified equations are following.

$$\begin{cases} -\nabla \cdot (\sigma \nabla u) = 0 & \text{in } \Omega \\ -\sigma \nabla u = g & \text{on } \partial\Omega \end{cases},$$

where $u(\mathbf{x})$ is a electrical potential, $\sigma(\mathbf{x})$ is a electrical conductivity, and $-\sigma \nabla u(= \mathbf{J})$ is a current density(current passing through unit volume). The objective function is $\sigma(\mathbf{x})$, provided \mathbf{J} or magnetic field density \mathbf{B} , particularly only component B_z .

This kind of equation actually is very abundant in various modeling, it will not be just a electrical progress to resolve that inverse problem but many equilibrium model or diffusive model. In view of this, It was not a brand new approach to approximate it as a discrete network model[21], there are many instances in area mechanical force balancing, or even in electrical model. So we introduce electrical network approach here in connection with finite difference or integral form of equations, and how it will solve them. This will provide simplified framework in the relation between \mathbf{J} , B_z , σ . In the first chapter, we introduce about MREIT, in 2nd chapter, we give a brief history on MREIT problem since 1992. In 3rd chapter, we connect our network approach to the others' research and try to give linearized explanation. In 4th chapter, we report our result of numerical simulation using network approach. We are going to mention that it is very stable to noise and solved very nice and fast way.

Contents

Abstract	i
Contents	iii
List of Figures	iv
1 Introduction	1
2 History	3
2.1 1992 ~ 2003	3
2.2 2003 ~	5
3 Rank explanation with network approach	9
3.1 \mathbf{J} recovery in Park's[17] paper	9
3.1.1 Explanation	9
3.2 Integral form of MREIT	10
3.3 Introduction to network approach	14
3.3.1 Kirchoff's Laws, curl of Ampere's Law	15
3.3.2 Counting Network Variables	15
3.4 Rank explanation with network approach	17
3.4.1 Rank sufficiency in 3D with \mathbf{J}	17
3.4.2 Rank deficiency in 3D with B_z	17
3.4.3 Rank sufficiency in 2D with B_z	17
3.4.4 Rank sufficiency in 3D with $B_z, J_z = 0$	18
3.4.5 Rank sufficiency in 3D with B_z for projected current	18
4 Simulation of Network Approach	20
4.1 Problem definition	20
4.2 2D cases	21
4.2.1 2D isotropic conductivity	22
4.2.2 2D semi-anisotropic conductivity	25

4.3	3D cases	30
4.3.1	3D Isotropic conductivity	31
4.3.2	3D semi-anisotropic case	32
5	Conclusions	37
6	Appendix : Stability analysis	38
	Summary (in Korean)	40
	References	41

List of Figures

3.1	small square domain S	11
3.2	Resistive Networks	15
4.1	A continuous conductivity body is discretized using a resistive network. Then the backward solver is given by the Kirchhoff's voltage (or circuit) law.	22
4.2	Two dimensional isotropic conductivity has been recovered under three different injection currents. Injection currents are denoted by arrows. The best result is (c). In this example noise levels are all zero.	23
4.3	This is an example that the discontinuity of the conductivity is orthogonal to the main stream of the current. Since the boundary conductivity is assumed to be given, the conductivity is reasonably recovered even with 25% of noise.	25
4.4	Isotropic conductivity recovery in two dimensional space. The noise level is increased up to 25%.	26
4.5	Two dimensional semi-isotropic conductivity images obtained as increasing the number of given boundary layers from 2 to 8. The noise level is 5%. The images in the second row are of horizontal resistors a_{ij} 's and the ones in the third row are for b_{ij} 's.	27
4.6	Two dimensional semi-isotropic conductivity images obtained as increasing the number of input nodes from 10 to 40. For example, five input nodes were used to each of two parallel sides which totals ten input nodes. The noise level in this example is 10%.	29
4.7	A cell of a three dimensional resistive Network	30
4.8	Isotropic conductivity image in three dimension. Injection current for the first row is given through two points $(0, 0, 0)$ and $(1, 1, 1)$. The second row uses $(1, 0, 1)$ and $(0, 1, 0)$ and the third one uses $(0, 1, 0.5)$ and $(1, 0, 0.5)$	34
4.9	Three dimensional semi-anisotropic conductivity images. Two sets of injection currents are applied in the direction of x and y -axes. These figures are slices of three dimensional body orthogonal to the z -axis with $k = 68$ out of 128. The image for c_{ijk} is worse than others since the current in the direction is weaker.	35

4.10 Three dimensional semi-anisotropic conductivity images. Two sets of injection currents are applied in the direction of x and y -axes. These figures are slices of three dimensional body orthogonal to the x -axis with $i = 60$ out of 128 layers. The actual conductivity is range is $1 \leq \sigma \leq 5$. The noise level of this example is 10%. 36

1. Introduction

We start with typical configuration of EIT problem and later MREIT problem. Electrical relation of internal body can be formulated as following dirichilet problem.

$$\begin{cases} -\nabla \cdot (\sigma \nabla u) = 0 & \text{in } \Omega \\ u = f & \text{on } \partial\Omega \end{cases} \quad (1.1)$$

$-\sigma \nabla u := \mathbf{J}$ is Ohm's law, σ is conductivity, ∇u is potential difference and \mathbf{J} is current density. The condition $\nabla \cdot (\sigma \nabla u) = 0$ is Kirchoff's current law or conservation law of electrical charge. Neumann problem configuration is also possible. In 1.1, we say forward problem as for given boundary condition f and coefficient σ , finding out the solution u . The backward problem or inverse problem is that finding out coefficient σ , for given one or more pair of f and u of boundary conditions and solutions. So we call it as a EIT problem, an inverse problem, that finding out conductivity of internal body by measuring only boundary voltages.

However EIT problem can hardly be solved in high resolution because using only boundary information causes ill-posedness in problem. So there were difficulties in EIT and now it is mainly used as anomaly detection that we only need low resolution and low cost.

In the meantime, there was another effort to get internal body image, the MRCDI. This is basically based on the Ampere's law $\mathbf{J} = \nabla \times \mathbf{B}/\mu_0$. We can obtain the current density image from given magnetic field density \mathbf{B} via taking curl operator on it. The magnetic field density \mathbf{B} is given by MRI. MRI machine provides magnetic field density of each slice which is normal to the particular axis. Therefore, since we need whole three component of (B_x, B_y, B_z) , in order to get \mathbf{J} , we should rotate and measure the body three times without any shake and this can be a non-trivial obstacle in practical treatment.

In view of concerning EIT problem, the informations available through non-destructive way, i.e. not to open or impulse the body, are not only boundary voltages, but also the internal current density. We can make use of internal information that MRCDI gives via MRI. The costs increased here are only in economical when using MRI, but feasibility is not a problem technically. In fact, It is a good few informations to start with to resolve problem mathematically that we have already internal current density so we expect somehow its well-posedness and not great complexity. Now we have internal current density then, if we are known the internal voltage map also by a certain mechanism, or by adding more relations,

we may acquire the conductivity σ by Ohm's law or other relations.

So now we formulate MREIT problem that is EIT based on internal current density \mathbf{J} below. The neumann problem configurations are following.

$$\begin{cases} -\nabla \cdot (\sigma \nabla u) = 0 & \text{in } \Omega \\ -\sigma \nabla u = g & \text{on } \partial\Omega \end{cases} \quad (1.2)$$

The MREIT problems in above are

MREIT Problem. *for given one or more (\mathbf{J}, g) pair, find out the conductivity σ in Ω*

MREIT Problem. *for given one or more (B_z, g) pair, find out the conductivity σ in Ω*

MREIT problem based on B_z is introduced in next chapter.

2. History

2.1 1992 ~ 2003

We briefly look inside of history of MREIT since 1992. Since there is a recent paper in 2008 May by Woo[23] which contains almost all references and materials of MREIT, we center important papers here introducing their issues.

According to the 2008 Woo[23], the first to approach EIT based on current density using MRI was Zhang in 1992[24], and 1994 Woo[22] and 1995 Birgul and Ider[1] also carried out research independently.

We first look up the paper 1994 Woo[22]. In general, \mathbf{J} and u are not linear about change of σ . This is contrast that \mathbf{J} , u are linear about change of voltage sources or current sources. So we can detect linearly by the change of \mathbf{J} the change of those sources, but we can't with σ . We should deal with ill-posedness due to non-linearity. However an early researchers started by trying to detect change of σ by measuring change of \mathbf{J} . $\Delta\sigma_i$, the change of σ at i -th local part is approximated by linear change \mathbf{J}_j at each local part. In other words, by the sensitivity matrix S , they tried the model $\mathbf{J}_j = S\Delta\sigma_i$. In this model, Woo suggested following algorithm. Let $\hat{\mathbf{J}}$ be a true given current density. We firstly set conductivity by guessing and solve the forward problem to get the computed current density \mathbf{J} . They expected that conductivity that produce computed current \mathbf{J} mostly close to the true current $\hat{\mathbf{J}}$ should close to true conductivity. According to sensitivity matrix model, we may update guessed conductivity by computing suitable local change of $\Delta\sigma_i$ so that updated conductivity produces current \mathbf{J} more closer to $\hat{\mathbf{J}}$ and moreover, we estimate the closedness by measuring $\|\hat{\mathbf{J}} - \mathbf{J}\|_2$ in Ω . So we update conductivity, solve forward problem, and iterate this procedure and expect conductivity to converge to true conductivity producing almost close current to $\hat{\mathbf{J}}$.

We now see the Kwon's 2002 J-substitution method[7] that overcome almost all drawback of Woo's method and 2003 Kim[6] that proves uniqueness and discusses about convergence. If we investigate Woo's method rigorously, firstly \mathbf{J} is not linear to σ , secondly the conductivity that produce same current density is not unique, thirdly we can't assure the convergence for all cases. About non-uniqueness problem, just think of material whose conductivities are distributed parallelly to each other that are all perpendicular to the current passing direction. The current can't notice the change of conductivity in their passway.

In J-substitution method, they updated conductivity not by sensitivity matrix model, but by Ohm's law. The procedures are like this. Set conductivity initially by guessing and solve forward problem to get the potential ∇u . Since we know true current $\hat{\mathbf{J}}$, we can update conductivity by $\sigma_{next} = \frac{|\hat{\mathbf{J}}|}{|\nabla u|}$, which is Ohm's law.

In order to avoid non-uniqueness, J-substitution method uses two sets of experimental true current \mathbf{J}^1 and \mathbf{J}^2 . \mathbf{J}^1 and \mathbf{J}^2 are configured to have following condition a.e. in Ω by injecting boundary current exclusively.

$$|\mathbf{J}^1 \times \mathbf{J}^2| \neq 0 \quad (2.1)$$

Kim[6] proved that the conductivity is unique which produces same such two sets of current. J-substitution method implemented this by setting two different boundary conditions(injecting currents) in each iterate's forward problem alternatively and update σ by two different true currents $\hat{\mathbf{J}}_1, \hat{\mathbf{J}}_2$ alternatively. The convergence issues are discussed in Kim[6]

J-substitution method is evaluated to have a practical feasibility, but it still needs to guarantee stability to noise and it takes cost to solve forward problem in each iterate. Computation time is shown increased rapidly, in 2003 Lee[11] p.1980, due to rapid increasing of unknowns in 3D problem. This could be another technical obstacle in practical medical treatment.

Kwon 2002[8] suggested another approach to this problem. We discussed already that taking sufficient advantages of knowing internal information is probably needed in algorithm. Kwon uses a kind of characteristic method to reduce internal potential value to boundary potential value which is measurable. The following fact are used that equipotential lines are always perpendicular to the direction of current. This induces following linear differential equation.

$$\begin{aligned} \frac{dX_t}{ds}(s) &= \left(\frac{J(X_t(s))}{|J(X_t(s))|} \right)^\perp \\ X_t(0) &= x_t, \quad X_t(s_f) \in \partial\Omega, \end{aligned} \quad (2.2)$$

where $X_t(0) = x_t$ is an internal interesting point and $X_t(s_f)$ is a final point at boundary. The values of potentials are same along equipotential line and one of them belongs to the boundary. So now we have internal potential information and internal current information, by Ohm's law, we obtain internal conductivity. All details of this method are well developed in Kwon[8] in cases conductivity is continuous or discontinuous and case there is a point that passing current is zero. Equipotential line method became successfully supported by mathematics. Meanwhile, the fact that equipotential lines are always perpendicular to stream of current cannot be applied if conductivity is anisotropic tensor.

In 2003, Ider suggested non-iterative method[4] that is shown in Woo's method and J-substitution. Ider just recover conductivity by solving a linear system of equations once and integrate it. This method is based on the curl-free condition of potential, i.e. $\nabla \times (\nabla u) = 0$. From this we obtain followings.

$$\nabla \times (\nabla u) = 0 \quad (2.3)$$

$$\nabla \times \frac{\mathbf{J}}{\sigma} = 0 \quad (2.4)$$

$$\nabla \rho \times \mathbf{J} + \rho \nabla \times \mathbf{J} = 0, \quad \rho = \frac{1}{\sigma} \quad (2.5)$$

$$\nabla \tau \times \mathbf{J} = -\nabla \times \mathbf{J}, \quad \tau = \log \rho, \quad \nabla \tau = \frac{\nabla \rho}{\rho} \quad (2.6)$$

In above, 2.6 is a linear system whose unknowns are $\nabla \tau$. If we write down all its components,

$$\begin{bmatrix} 0 & J_z & -J_y \\ -J_z & 0 & J_x \\ J_y & -J_x & 0 \end{bmatrix} \begin{bmatrix} \frac{\partial \tau}{\partial x} \\ \frac{\partial \tau}{\partial y} \\ \frac{\partial \tau}{\partial z} \end{bmatrix} = - \begin{bmatrix} \frac{\partial J_z}{\partial y} - \frac{\partial J_y}{\partial z} \\ \frac{\partial J_x}{\partial z} - \frac{\partial J_z}{\partial x} \\ \frac{\partial J_y}{\partial x} - \frac{\partial J_x}{\partial y} \end{bmatrix} \quad (2.7)$$

and we notice that the rank of this system is only 2. Hence, we use two sets of data, we can solve for $\nabla \tau(\mathbf{r})$ for each point. If we are given some amount of conductivity on boundary, conductivity at internal point \mathbf{r} can be attained by integrate $\nabla \tau(\mathbf{r})$ over grid line or general line connecting the certain boundary point to it. This kind of non-iterative method shows very clear process so the method is revealed to have a stability to multiplicative noise.

2.2 2003 ~

We discussed the fact that we need three times measurement of rotated body to obtain $\mathbf{J} = \nabla \times (B_x, B_y, B_z)$. In the purpose of overcome this difficulty, they tried to pull out information from only in one component of magnetic field density B_z as much as possible not to make a new MRI-like machine. Also people wanted to know what is inferred exactly and what is lost exactly. So 2003 Seo[20], 2006 Kwon[10] and [17] investigate these questions.

We can formulate it as B_z -based MREIT problem.

MREIT Problem. *for given one or more (B_z, g) pair, find out the conductivity σ in $\Omega \in \mathbb{R}^3$*

The first of these approach is said to be very early paper 1995 Birgul and Ider[1]. However it seems this is due to their model was 2-dimensional problem of slices of 3D domain. It seems people found a clue in a early stage research after long time.

In such a context, we look up 2003 Seo[19], Seo[20], Oh[14]. They suggested the Harmonic- B_z algorithm in Seo[19] and Oh[14]. This uses the relation below.

$$\frac{1}{\mu_0} \nabla^2 B_z(\mathbf{r}) = -\frac{\partial J_x}{\partial y} + \frac{\partial J_y}{\partial x} = -\tilde{\nabla} \times (J_x, J_y)(\mathbf{r}) \quad (2.8)$$

$$= \left(\frac{\partial \sigma}{\partial x}, \frac{\partial \sigma}{\partial y} \right) \cdot \left(\frac{\partial u}{\partial y}, -\frac{\partial u}{\partial x} \right), \quad (2.9)$$

$$\text{where } \tilde{\nabla} = \left(\frac{\partial}{\partial x}, \frac{\partial}{\partial y} \right) \quad \text{2D x-y plane grad} \quad (2.10)$$

If the term $\left(\frac{\partial u}{\partial y}, -\frac{\partial u}{\partial x} \right)$ is known, then we can put them as coefficients so the equation becomes linear equation at each point \mathbf{r} , and by using two sets of data, we solve 2 by 2 system to get unknowns $\left(\frac{\partial \sigma}{\partial x}, \frac{\partial \sigma}{\partial y} \right)$. Similarly in Ider's method, we can recover internal conductivity by integrate those terms from boundary point to it. This process can be viewed more intuitively by network model in next chapter. After for a while, they integrate those terms via layer-potential technic.

However, $\left(\frac{\partial u}{\partial y}, -\frac{\partial u}{\partial x} \right)$ are not known coefficients but depend on unknown σ . The problem becomes non-linear so they suggested iterative algorithm analogous to J-substitution and named it Harmonic- B_z algorithm. Many experiments are performed under this framework.

When we make use of \mathbf{J} , we noticed that the problem is closed. The papers before and the analysis in next chapter can show this so this aspect enables the non-iterative method. Since we are now using B_z only, we have informations in lost and it is revealed not so much trivial but a certain enough amount of informations that the problem is not closed anymore. Without additional assumptions, we may not avoid iterative way and explanation of these aspects are in next chapter.

Accordingly, Seo[20] consider only domains which are not so much thick in z -axis so that conductivity is distributed cylindrically, i.e.

$$\Omega_s = D \times (-\delta, +\delta) \quad (2.11)$$

We set boundary injecting current suitably so that we can assume the transversal current J_z is zero. In this configuration, \mathbf{J} can be recovered from B_z . We make use of the condition $\nabla \cdot \mathbf{J} = 0$ and the Biot-Savart's law.

$$\nabla \cdot \mathbf{J} = 0 \quad \mathbf{r} \in \Omega_s \quad (2.12)$$

$$B_z(\mathbf{r}) = \frac{\mu_0}{4\pi} \int_{\Omega} \frac{(y-y')J_x(\mathbf{r}') - (x-x')J_y(\mathbf{r}')}{|\mathbf{r}-\mathbf{r}'|^3} d\mathbf{r}' \quad \mathbf{r} \in \Omega_s \quad (2.13)$$

First, since $J_z = 0$, the 3D divergence-free condition $\nabla \cdot \mathbf{J} = 0$ is equivalent to 2D divergence-free condition $\tilde{\nabla} \cdot (J_x, J_y) = 0$, hence 2D form can be available.

Another one, Biot-Savart's law expands in interested domain Ω_s like this.

$$B_z(\mathbf{r}) = \frac{\mu_0}{4\pi} \int_{\Omega_s} \frac{(y-y')J_x(\mathbf{r}') - (x-x')J_y(\mathbf{r}')}{|\mathbf{r}-\mathbf{r}'|^3} d\mathbf{r}' + G(\mathbf{r}) + B_z^I(\mathbf{r}) \quad \mathbf{r} \in \Omega_s \quad (2.14)$$

$B_z^I(\mathbf{r})$ is magnetic field density exerting on Ω_s from outside of Ω by electrodes and $G(\mathbf{r})$ is magnetic field density exerting on Ω_s from outside $\Omega \setminus \Omega_s$ by currents at $\Omega \setminus \Omega_s$.

$$G(\mathbf{r}) = \frac{\mu_0}{4\pi} \int_{\Omega \setminus \Omega_s} \frac{(y-y')J_x(\mathbf{r}') - (x-x')J_y(\mathbf{r}')}{|\mathbf{r}-\mathbf{r}'|^3} d\mathbf{r}' \quad \mathbf{r} \in \Omega_s \quad (2.15)$$

Formulation of Biot-Savart's law raises the property that terms $B_z^I(\mathbf{r})$ and $G(\mathbf{r})$ exerting from outside of Ω_s vanishes as taking laplace operator on the equation and term due to domain itself is abstracted to curl of current. The results are following.

$$\nabla^2 B_z(\mathbf{r}) = -\mu_0 \tilde{\nabla} \times (J_x, J_y) \quad \mathbf{r} \in \Omega_s \quad (2.16)$$

This also can be identified from the vector identity $\nabla \times \nabla \times \mathbf{B} = \nabla(\nabla \cdot \mathbf{B}) - \nabla^2 \mathbf{B} = 0 - \nabla^2 \mathbf{B}$. So let's call it curl of Ampere's law. The left-hand-side of 2.16 is known value and about right-hand-side, we take advantage of 2D-divergence-free condition to represent \mathbf{J} as streamfunction $(\frac{\partial \beta}{\partial y}, -\frac{\partial \beta}{\partial x}, 0)$ so that right-hand-side would be $\mu_0 \nabla^2 \beta$. Hence this is well-known poisson equaton, we can compute the current \mathbf{J} and $J_z = 0$ assures that we've done for all current.

Meanwhile, Ider extended his non-iterative J-based method [4] to B_z -based method[5]. Owing to use B_z only, the scheme is iterative.

While people were conducting researches with B_z , It is required that complete and accurate analysis about this framework is required and In 2006 Kwon[10] and 2007 Park[17] deal with these questions. 2006 Kwon proved uniqueness in a slice normal to z -axis as a 2D problem and proved analogously in a 3D domain assuming domain is cylindrical extension of the slice like in 2.11.

2007 Park answered the questions of what is the most recoverable informations and what is lost exactly by presenting explicit recoverable currents. The paper defined the linear operator \mathcal{T} as,

$$\mathcal{T} : \mathbf{J} \longmapsto (\nabla^2 B_z, \mathbf{J} \cdot \mathbf{n}) \quad (2.17)$$

where the values $\nabla^2 B_z$ are in Ω and the values $\mathbf{J} \cdot \mathbf{n}$ are in $\partial\Omega$. The kernel of this linear operator is exactly what we lost and mapped element \mathbf{J}^P is the very current recoverable mostly. In detatil, the paper proved that the elements \mathbf{J}^D in the $Ker \mathcal{T}$ are the elements that make up 2D curl-free part of current at each slices, i.e. $\tilde{\nabla} \times \mathbf{J}^D = 0$ and we don't pose any boundary current injecting condition there. They also proved that \mathbf{J}^P is the sum of

two terms, one makes up 3D curl-free part of current. We pose whole boundary injecting current condition here and denote \mathbf{J}^0 . The other one makes up the part that 2D curl values are given as $-\frac{1}{\mu_0}\nabla^2 B_z$ at each slices and denote this \mathbf{J}^* . We will give more explanation in the next chapter. Therefore, we know explicitly what is gained and what is lost. The recovered current \mathbf{J}^P , not assuming $\mathbf{J} = 0$ is called projected current. Moreover, they estimated the difference between true current and projected current $\|\mathbf{J} - \mathbf{J}^P\|$ by $\|J_z - J_z^0\|$ and $\|\frac{\partial J_z^0}{\partial z} - \frac{\partial J_z}{\partial z}\|$. We can see \mathbf{J} would be almostly recoverable if true J_z is not so much big that does not generate any curl part and \mathbf{J} does not vary much in z -direction.

The effort to recover conductivity with this projected currents was conducted by 2008 Nam[13]. Since we start with current \mathbf{J}^P , not B_z , this method is non-iterative. In Nam's paper, actually, they do not compute \mathbf{J}^P but recover σ directly from B_z with whole above relations and harmonic- B_z relation 2.16. This is only different in whether find out whole unknowns \mathbf{J}, σ or firstly solve for \mathbf{J} and replace it to solve for σ .

3. Rank explanation with network approach

We introduced several approaches to recover \mathbf{J} and σ from B_z , or B_z with additional assumption. In this chapter, we particularly look inside the contents in 2007 Park[17]. The last purpose is to explain what are the counter parts of those in network model and express them in network terms which is more linearized explanation.

3.1 J recovery in Park's[17] paper

The recovered current \mathbf{J}^P in Park's paper is following.

$$\mathbf{J}^P = \mathbf{J}^0 + \mathbf{J}^* \quad (3.1)$$

$$= \nabla\alpha + \left(\frac{\partial\beta}{\partial y}, -\frac{\partial\beta}{\partial y}, 0 \right), \quad (3.2)$$

where α satisfies

$$\begin{aligned} \nabla^2\alpha &= 0 && \text{in } \Omega \\ \nabla \cdot \mathbf{n} &= \mathbf{J} \cdot \mathbf{n} && \text{on } \partial\Omega \quad \text{and} \quad \int_{\partial\Omega} \alpha ds = 0 \end{aligned} \quad (3.3)$$

and $\beta_t := \beta(x, y, t)$ satisfies in each slice Ω_t

$$\begin{aligned} \tilde{\nabla}^2\beta_t &= \frac{1}{\mu_0}\nabla^2 B_z && \text{in } \Omega_t \\ \beta_t &= 0 && \text{on } \partial\Omega_t \end{aligned} \quad (3.4)$$

Moreover, the missing part $\mathbf{J}^D = \mathbf{J} - \mathbf{J}^P$ satisfies,

$$\tilde{\nabla} \times (J_x^D, J_y^D) = 0 \quad \text{in } \Omega_t \quad \text{for all } t \in (-\delta, \delta)$$

3.1.1 Explanation

Intrinsically, current is divergence-free, i.e. $\nabla \cdot \mathbf{J} = 0$ and current also satisfies relation $\nabla \times \mathbf{J} = -\frac{1}{\mu_0}\nabla^2\mathbf{B}$. Therefore, we consider the following set of equations,

$$\begin{aligned} &\mathbf{J} \text{ satisfies} \\ &\left\{ \begin{array}{ll} \nabla \cdot \mathbf{J} &= 0 && \text{in } \Omega \\ \nabla \times \mathbf{J} &= -\frac{1}{\mu_0}\nabla^2\mathbf{B} && \text{in } \Omega \\ \mathbf{J} \cdot \mathbf{n} &= g && \text{on } \partial\Omega \end{array} \right. \quad (3.5) \end{aligned}$$

We decompose \mathbf{J} into curl-free part and remained part as,

$$\mathbf{J} = \mathbf{J}_{dfree+cfree} + \mathbf{J}_{dfree} \quad \text{satisfies} \quad \begin{cases} \nabla \cdot \mathbf{J}_{dfree+cfree} = 0 & \text{in } \Omega \\ \nabla \times \mathbf{J}_{dfree+cfree} = 0 & \text{in } \Omega \\ \mathbf{J}_{dfree+cfree} \cdot \mathbf{n} = g & \text{on } \partial\Omega \end{cases} \quad \begin{cases} \nabla \cdot \mathbf{J}_{dfree} = 0 & \text{in } \Omega \\ \nabla \times \mathbf{J}_{dfree} = -\frac{1}{\mu_0} \nabla^2 \mathbf{B} & \text{in } \Omega \\ \mathbf{J}_{dfree} \cdot \mathbf{n} = 0 & \text{on } \partial\Omega \end{cases} \quad (3.6)$$

Again, decompose \mathbf{J}_{dfree} into 2D divergence-free part on each (x, y) slices and remained part,

$$\mathbf{J} = \mathbf{J}_{dfree+cfree} + \mathbf{J}_{dfree(x,y)} + \mathbf{J}_{dfree+cfree(z)} \quad \text{satisfies} \quad \begin{cases} \nabla \cdot \mathbf{J}_{dfree+cfree} = 0 & \text{in } \Omega \\ \nabla \times \mathbf{J}_{dfree+cfree} = 0 & \text{in } \Omega \\ \mathbf{J}_{dfree+cfree} \cdot \mathbf{n} = g & \text{on } \partial\Omega \end{cases}$$

$$\begin{cases} \nabla \cdot \mathbf{J}_{dfree(x,y)} = 0 & \text{in } \Omega \\ \tilde{\nabla}_{(x,y)} \times \mathbf{J}_{dfree(x,y)} = -\frac{1}{\mu_0} \nabla^2 B_z & \text{in } \Omega \\ \tilde{\nabla}_{(y,z)} \times \mathbf{J}_{dfree(x,y)} = f & \text{in } \Omega \\ \tilde{\nabla}_{(z,x)} \times \mathbf{J}_{dfree(x,y)} = g & \text{in } \Omega \\ \mathbf{J}_{dfree(x,y)} \cdot \mathbf{n} = 0 & \text{on } \partial\Omega \end{cases} \quad (3.7)$$

$$\begin{cases} \nabla \cdot \mathbf{J}_{dfree+cfree(z)} = 0 & \text{in } \Omega \\ \tilde{\nabla}_{(x,y)} \times \mathbf{J}_{dfree+cfree(z)} = 0 & \text{in } \Omega \\ \tilde{\nabla}_{(y,z)} \times \mathbf{J}_{dfree+cfree(z)} = -\frac{1}{\mu_0} \nabla^2 B_x - f & \text{in } \Omega \\ \tilde{\nabla}_{(z,x)} \times \mathbf{J}_{dfree+cfree(z)} = -\frac{1}{\mu_0} \nabla^2 B_y - g & \text{in } \Omega \\ \mathbf{J}_{dfree+cfree(z)} \cdot \mathbf{n} = 0 & \text{on } \partial\Omega \end{cases}$$

Since $\mathbf{J}_{dfree+cfree}$ is curl-free, we express this with scalar potential $\nabla\alpha$ and $\nabla^2\alpha = 0$ because it is also divergence-free. In addition, we pose whole boundary condition to this term. This term $\mathbf{J}_{dfree+cfree}$ is the very \mathbf{J}^0 in previous section. Also, $\mathbf{J}_{dfree+cfree(z)}$ can be expressed with stream function $\left(\frac{\partial\beta}{\partial y}, -\frac{\partial\beta}{\partial x}, 0\right)$ since it is 2D divergence-free. So the curl-relation is written by $\tilde{\nabla}_{(x,y)} \times \mathbf{J}_{dfree+cfree(x,y)} = -\nabla^2\beta = -\frac{1}{\mu_0} \nabla^2 B_z$. We do not pose any boundary condition here. This term is the \mathbf{J}^* before. The remained is \mathbf{J}^D , we see $\tilde{\nabla}_{(x,y)} \times \mathbf{J}^D = 0$ above.

3.2 Integral form of MREIT

In this section, we consider integral form of the relations we've been used 2.4, 2.13 and 2.16 for purpose to express them in appropriate form that is fit with network model. Let's denote

the small square domain S in figure 3.2 with \square . S is a set on the one slice of Ω . The integral form of the left-hand-side in curl of Ampere's law 2.16 is,

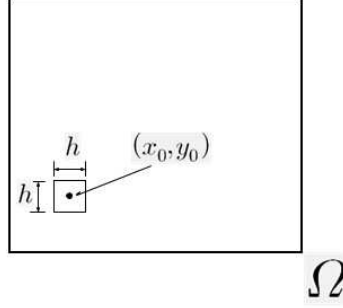


Figure 3.1: small square domain S

$$\int_{\square} \tilde{\nabla}_{(x,y)} \times \mathbf{J} dS = \int_{\partial \square} \mathbf{J} \cdot d\mathbf{s} \quad (3.8)$$

$$= \int_{x_0-h/2}^{x_0+h/2} J_x|_{(x,y_0-h/2)} dx + \int_{y_0-h/2}^{y_0+h/2} J_y|_{(x_0+h/2,y)} dy \\ + \int_{x_0+h/2}^{x_0-h/2} J_x|_{(x,y_0+h/2)} dx + \int_{y_0+h/2}^{y_0-h/2} J_y|_{(x_0+h/2,y)} dy \quad (3.9)$$

$$= \int_{x_0-h/2}^{x_0+h/2} J_x|_{(x,y_0-h/2)} dx + \int_{y_0-h/2}^{y_0+h/2} J_y|_{(x_0+h/2,y)} dy \\ - \int_{x_0-h/2}^{x_0+h/2} J_x|_{(x,y_0+h/2)} dx - \int_{y_0-h/2}^{y_0+h/2} J_y|_{(x_0+h/2,y)} dy \quad (3.10)$$

$$= J_x(c_1, y_0 - h/2)h + J_y(x_0 + h/2, c_2)h - J_x(c_3, y_0 + h/2)h - J_y(x_0 - h/2, c_4)h \quad (3.11)$$

. Stokes' theorem is used in first equality, mean value theorem is used in last equality with assuming $\mathbf{J} \in C^1(\Omega)$. Let's just assume that for a while. The right-hand-side of 2.16 is,

$$\int_{\square} -\frac{1}{\mu_0} \nabla^2 \mathbf{B}_z dS = -\frac{1}{\mu_0} \int_{\partial \square} \nabla \mathbf{B}_z \cdot \mathbf{n} ds \quad (3.12)$$

$$= -\frac{1}{\mu_0} \left(-\int_{x_0-h/2}^{x_0+h/2} \frac{\partial B_z}{\partial y} \Big|_{(x, y_0-h/2)} dx + \int_{y_0-h/2}^{y_0+h/2} \frac{\partial B_z}{\partial x} \Big|_{(x_0+h/2, y)} dy \right. \\ \left. + \int_{x_0-h/2}^{x_0+h/2} \frac{\partial B_z}{\partial y} \Big|_{(x, y_0+h/2)} dx - \int_{y_0-h/2}^{y_0+h/2} \frac{\partial B_z}{\partial x} \Big|_{(x_0+h/2, y)} dy \right) \quad (3.13)$$

$$= -\frac{1}{\mu_0} \left(\frac{\partial B_z}{\partial y}(d_1, y_0 - h/2)h + \frac{\partial B_z}{\partial x}(x_0 + h/2, d_2)h \right. \\ \left. - \frac{\partial B_z}{\partial y}(d_3, y_0 + h/2)h - \frac{\partial B_z}{\partial x}(x_0 - h/2, d_4)h \right). \quad (3.14)$$

Divergence theorem is used in first equality and we put only x, y terms of B_z here because $\frac{\partial B_z}{\partial z} = 0$ in the 2D plane. In last equality, we assumed $\mathbf{B} \in C^2(\Omega)$ and expressed using mean value theorem. In addition, Taylor expansion of $\frac{\partial B_z}{\partial y}$,

$$-\frac{\partial B_z}{\partial y}(d_1, y_0 - h/2) = \frac{(B_z(d_1, y_0 - h) - B_z(d_1, y_0))}{h} + \mathcal{O}\left(\frac{\partial^2 B_z}{\partial y^2} h^2\right) \quad (3.15)$$

$$= \frac{(B_z(x_0, y_0 - h) - B_z(x_0, y_0))}{h} + \mathcal{O}\left(\left(\frac{\partial^2 B_z}{\partial y^2} + \frac{\partial B_z}{\partial x}\right) h^2\right) \quad (3.16)$$

We again used \mathbf{B} is sufficiently smooth function. The whole terms similarly becomes,

$$\int_{\square} -\frac{1}{\mu_0} \nabla^2 \mathbf{B}_z dS \sim -\frac{1}{\mu_0} (B_z(x_0, y_0 - h) + B_z(x_0 + h, y_0) + B_z(x_0, y_0 + h) + B_z(x_0 - h, y_0) - 4B_z(x_0, y_0)). \quad (3.17)$$

This may be viewed as discretization of laplace operator in finite difference.

Hence, the curl of Ampere's law,

$$\int_{\partial \square} \mathbf{J} \cdot d\mathbf{s} = -\frac{1}{\mu_0} \int_{\partial \square} \nabla B_z \cdot \mathbf{n} ds \quad (3.18)$$

is written by,

$$J_x(c_1, y_0 - h/2)h + J_y(x_0 + h/2, c_2)h - J_x(c_3, y_0 + h/2)h - J_y(x_0 + h/2, c_4)h \\ = -\frac{1}{\mu_0} (B_z(x_0, y_0 - h) + B_z(x_0 + h, y_0) + B_z(x_0, y_0 + h) + B_z(x_0 - h, y_0) - 4B_z(x_0, y_0)). \quad (3.19)$$

This is algebraic equation about 4 current variables along circumference of square cell \square and 5 B_z variables on the center of each square cells.

Meanwhile, the integral form of $\nabla \times \nabla u = 0$ in square cell \square is,

$$\int_{\square} \tilde{\nabla} \times \nabla u dS = \int_{\square} \tilde{\nabla} \times -\frac{\mathbf{J}}{\sigma} dS \quad (3.20)$$

$$= \int_{\square} \tilde{\nabla} \times -\rho \mathbf{J} dS, \quad (\rho = \frac{1}{\sigma}) \quad (3.21)$$

$$= \int_{\partial \square} -\rho \mathbf{J} \cdot d\mathbf{s} \quad (3.22)$$

$$= \int_{x_0-h/2}^{x_0+h/2} -\rho J_x|_{(x,y_0-h/2)} dx + \int_{y_0-h/2}^{y_0+h/2} -\rho J_y|_{(x_0+h/2,y)} dy \\ + \int_{x_0+h/2}^{x_0-h/2} -\rho J_x|_{(x,y_0+h/2)} dx + \int_{y_0+h/2}^{y_0-h/2} -\rho J_y|_{(x_0+h/2,y)} dy \quad (3.23)$$

$$= \int_{x_0-h/2}^{x_0+h/2} -\rho J_x|_{(x,y_0-h/2)} dx + \int_{y_0-h/2}^{y_0+h/2} -\rho J_y|_{(x_0+h/2,y)} dy \\ - \int_{x_0-h/2}^{x_0+h/2} -\rho J_x|_{(x,y_0+h/2)} dx - \int_{y_0-h/2}^{y_0+h/2} -\rho J_y|_{(x_0+h/2,y)} dy \quad (3.24)$$

$$= -\rho(e_1, y_0 - h/2) J_x(e_1, y_0 - h/2) h - \rho(x_0 + h/2, e_2) J_y(x_0 + h/2, e_2) h \\ + \rho(e_3, y_0 + h/2) J_x(e_3, y_0 + h/2) h + \rho(x_0 - h/2, e_4) J_y(x_0 - h/2, e_4) h. \quad (3.25)$$

This is another algebraic equation.

Finally the integral form of $\nabla \cdot \mathbf{J}$ is,

$$\int_{\square} \nabla \cdot \mathbf{J} dS = \int_{\partial \square} \mathbf{J} \cdot \mathbf{n} ds \quad (3.26)$$

$$= \int_{x_0-h/2}^{x_0+h/2} -J_y|_{(x,y_0-h/2)} dx + \int_{y_0-h/2}^{y_0+h/2} J_x|_{(x_0+h/2,y)} dy \\ + \int_{x_0+h/2}^{x_0-h/2} J_y|_{(x,y_0+h/2)} dx - \int_{y_0-h/2}^{y_0+h/2} J_x|_{(x_0+h/2,y)} dy \quad (3.27)$$

$$= -J_y(e_1, y_0 - h/2) h + J_x(x_0 + h/2, e_2) h + J_y(e_3, y_0 + h/2) h - J_x(x_0 - h/2, e_4) h. \quad (3.28)$$

In order to jump to network model from continuous model, we pose two additional assumption. One is assumption that second derivative $|\mathbf{D}^2 \mathbf{J}|$ is not so big that we can locally approximate \mathbf{J} linearly. The other one is partial derivatives $|\frac{\partial J_x}{\partial x}| \ll |\frac{\partial J_x}{\partial y}|$ and similarly $|\frac{\partial J_y}{\partial y}| \ll |\frac{\partial J_y}{\partial x}|$. Concern about second assumption, this is not true in general, but the tendency was found in the numerical simulation and this needs more explanation how come we do that.

The left-hand-side of the 3.19, we use second assumption so that we treat J_x along very short x -line in \square as a constant compared with J_y . Hence, we express first term $\int_{x_0-h/2}^{x_0+h/2} J_x|_{(x,y_0-h/2)} dx \cong j_1 h$, which is constant in there. The whole equation are following.

$$\begin{aligned}
& j_1 h + j_2 h - j_3 h - j_4 h \\
= & -\frac{1}{\mu_0} (B_z(x_0, y_0 - h) + B_z(x_0 + h, y_0) + B_z(x_0, y_0 + h) + B_z(x_0 - h, y_0) - 4B_z(x_0, y_0))
\end{aligned} \tag{3.29}$$

This is a constant coefficients linear equation.

Secondly, in 3.25 $\nabla \times \nabla u = 0$ condition, we use second assumption again so the first integral $\int_{x_0-h/2}^{x_0+h/2} -\rho J_x|_{(x,y_0-h/2)} dx \cong j_1 \int_{x_0-h/2}^{x_0+h/2} -\rho dx$. Similarly,

$$\begin{aligned}
\int_{\square} \tilde{\nabla} \times \nabla u dS &= j_1 \int_{x_0-h/2}^{x_0+h/2} -\rho dx + j_2 \int_{y_0-h/2}^{y_0+h/2} -\rho dy \\
&\quad - j_3 \int_{x_0-h/2}^{x_0+h/2} -\rho dx - j_4 \int_{y_0-h/2}^{y_0+h/2} -\rho dy
\end{aligned} \tag{3.30}$$

$$= -j_1 \tilde{\rho}_1 + j_2 \tilde{\rho}_2 + j_3 \tilde{\rho}_3 - j_4 \tilde{\rho}_4. \tag{3.31}$$

we put $\int \rho$ also as a representative variable $\tilde{\rho} = \int \rho$ here. This is also a constant coefficients linear equation, .

Lastly, In 3.28 $\nabla \cdot \mathbf{J} = 0$ condition, we use first assumption so that \mathbf{J} is locally linear in S . The first integral $\int_{x_0-h/2}^{x_0+h/2} -J_y|_{(x,y_0-h/2)} dx \cong -J_y(x_0, y_0 - h/2)$. This value is just j_4 of the square translated by $(h/2, h/2)$. So this becomes also a constant coefficients linear equation. We've tried these approximations in purpose to assign continuous variables into network edge variables.

3.3 Introduction to network approach

Let's consider following discrete resistive network instead of continuous domain Ω . In resistive network, the current in a edge is not changed in there, resistivity is also represented by one value in there so the algebraic equations above are all linear. In this section, we mainly discuss the each counterpart of conditions $\nabla \cdot \mathbf{J} = 0$, $\nabla \times \nabla u$ and $\nabla^2 B_z(\mathbf{r}) = -\mu_0 \tilde{\nabla} \times (J_x, J_y)$ in resistive network. Also counting how many network variables such as nodes, edges and loops are presented.

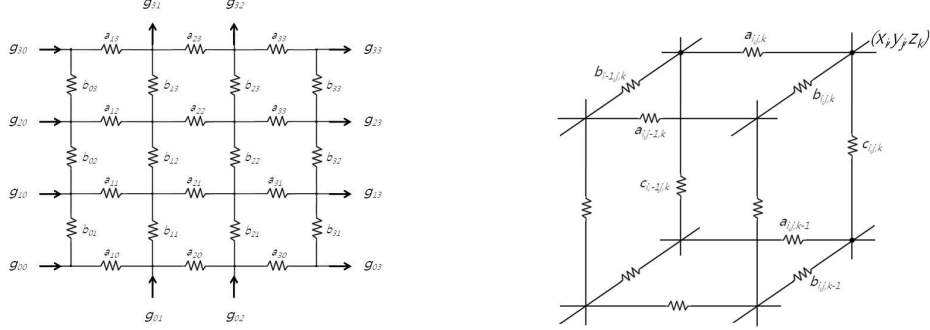


Figure 3.2: Resistive Networks

3.3.1 Kirchoff's Laws, curl of Ampere's Law

The conditions $\nabla \cdot \mathbf{J} = 0$ and $\nabla \times \nabla u$ are just Kirchoff's current law and voltage law in resistive network. These two laws and harmonic- B_z relation (or curl of Ampere's law) in network are connected to continuous problem by approximation of integral forms with additional assumptions as we discuss before.

The MREIT problem on these resistive networks are following.

MREIT Problem. for given one or more (\mathbf{J}, g) edge-variable pair, find out the edge-variable conductivity σ in Ω

MREIT Problem. for given one or more (B_z, g) edge-variable pair, find out the edge-variable conductivity σ in Ω

In continuous version, we solve partial differential equation to recover conductivity using the laws, on the other hand in discrete version, we solve a linear system of equations and each laws make up for each amount of ranks in the system.

3.3.2 Counting Network Variables

As in the Figure 3.2, we count network variables nodes, edges and loops. Potential u is node variable, current j and σ are edge variables. Loops are used in Kirchoff's voltage laws. For square grid in 2D or 3D, the total number of nodes are counted as,

$$\text{number of nodes} = n^2 \quad \text{in } 2D \quad (3.32)$$

$$\text{number of nodes} = n^3 \quad \text{in } 3D \quad (3.33)$$

On the other hand, the total number of edges are,

$$\text{number of edges} = 2n(n-1) \sim 2n^2 \quad \text{in } 2D \quad (3.34)$$

$$\text{number of edges} = 3n^2(n-1) \sim 3n^3 \quad \text{in } 3D \quad (3.35)$$

and for the loops which is applicable for any closed path, we only count linearly independent loops, i.e. loops that are representable with other loops' combination are not counted, hence we work with each cell's loop basically. Think of each cube cell in 3D, there are six faces and loops are available for each faces. Two faces are normal to x -axis, the other two faces are normal to y -axis, and the rest two faces are normal to z -axis. The loops of one direction are representable by those of the other two directions. Therefore the total number of linearly independent loops are below.

$$\text{number of loops} = (n-1)^2 \sim n^2 \quad \text{in } 2D \quad (3.36)$$

$$\text{number of loops} = 2n(n-1)^2 \sim 2n^3 \quad \text{in } 3D \quad (3.37)$$

For the ranks that each laws can fill up are counted below. Kirchhoff's current law(KCL) is applied to each nodes and Kirchhoff's voltage law(KVL) is applied to each loops. 2D curl of Ampere's law is applied to loops on each slices.

$$2D \text{ KCL} \sim n^2 \quad (3.38)$$

$$2D \text{ KVL} \sim n^2 \quad (3.39)$$

$$3D \text{ KCL} \sim n^3 \quad (3.40)$$

$$2D \text{ KVL} \sim 2n^3 \quad (3.41)$$

$$2D \text{ curl of Ampere's law} \sim n^3 \quad (3.42)$$

The total number of unknowns σ or σ, j are same as that of edges each.

For example, consider the simplest constitution of MREIT problem that 2D \mathbf{J} is given in network. To determine the $2n^2$ of unknowns σ , available law is Kirchhoff's voltage law only. Kirchhoff's current law is for validating given current j . The total available equations are n^2 which lack half of required. Therefore we employ two sets of current data, we can solve them under condition all equations in them are linearly independent to each other. This condition is seen at 2.1 before, and the uniqueness of network version is therefore consistent with that of continuous version using two such sets of data on Kim[6]. We investigate other constitutions.

3.4 Rank explanation with network approach

3.4.1 Rank sufficiency in 3D with \mathbf{J}

3D case for given j , we can solve.

- Unknowns
 - $\sigma \sim 3n^3$

available equations are,

- Equations
 - KVL $\sim 2n^3 \times 2$

as you can see, system becomes over-determined.

3.4.2 Rank deficiency in 3D with B_z

3D case for given B_z , unknowns are as below.

- Unknowns
 - $\sigma \sim 3n^3$
 - $\mathbf{J} \sim 3n^3 \times 2$

available equations are,

- Equations
 - curl of Ampere's law $\sim n^3 \times 2$
 - KVL $\sim 2n^3 \times 2$

So here, network model reflect that we cannot close problem only with B_z . Hence iterative schemes have been used in continuous version.

3.4.3 Rank sufficiency in 2D with B_z

2D case for given B_z , we can solve.

- Unknowns
 - $\sigma \sim 2n^2$

- $\mathbf{J} \sim 2n^2 \times 2$

- Equations

- curl of Ampere's law $\sim n^2 \times 2$

- 2D KVL $\sim n^2 \times 2$

- 2D KCL $\sim n^2 \times 2$

This is consistent with the result of 2006 Kwon[10].

3.4.4 Rank sufficiency in 3D with $B_z, J_z = 0$

2003 Seo[20] recovered \mathbf{J} by using B_z with additional condition $J_z = 0$. Unknowns for this case that are interested are only edges in (x, y) -plane, not in z -axis. So latter are not counted for unknowns. Also 3D KCL are available in this case.

- Unknowns

- $\sigma \sim 2n^3$

- $\mathbf{J} \sim 2n^3 \times 2$

- Equations

- curl of Ampere's law $\sim n^3 \times 2$

- KVL $\sim n^3 \times 2$

- KCL $\sim n^3 \times 2$

Network model reflect the number of ranks are enough to solve system and so did in continuous version in Seo's paper. In view of this, employeed Harmonic- B_z or J-substitution are redundant when assuming $J_z = 0$.

3.4.5 Rank sufficiency in 3D with B_z for projected current

Last case recover \mathbf{J}^P, σ from B_z .

- Unknowns

- $\sigma \sim 3n^3$

- $\mathbf{J}^0 \sim 3n^3 \times 2$

- $\mathbf{J}^* \sim 2n^3 \times 2$

- Equations

- 3D KVL $\sim 2n^3 \times 2$
- 2D KCL of $\mathbf{J}^0 \sim n^3 \times 2$
- 2D KVL of $\mathbf{J}^0 \sim 2n^3 \times 2$
- 3D KCL of $\mathbf{J}^* \sim n^3 \times 2$
- curl of Ampere's law of $\mathbf{J}^* \sim n^3 \times 2$

z -direction edges can also be ignored as in case before, then equations in z -direction KVL also are removed. Since KVL using projected current are also in approximation sense, this constitution seems more reasonable. Again, we recover \mathbf{J}^P in this case, so the problem is closed and can be solved by non-iterative scheme as in 2008 Nam[13].

4. Simulation of Network Approach

In this chapter, we present numerical simulation of network approach for configurations given \mathbf{J} in 2D and 3D cases. Large part of this chapter is the testing stability to noise of this method and also there will be several reported properties of this method.

4.1 Problem definition

The detail configuration of problem this simulation conducted are followings.

MREIT Problem. • *for given one or more (\mathbf{J}, g) edge-variable pair, find out the edge-variable conductivity σ in Ω ,*

- *Ω is rectangular 2D or 3D domain,*
- *We assume that the conductivity tensor σ is bounded and positive definite, i.e., there exists known positive constants c_0 and C_0 such that*

$$0 < c_0 \leq \sigma \leq C_0 < \infty \text{ in } \Omega. \quad (4.1)$$

- *The conductivity σ is also assumed to be given in some part of the boundary, i.e.,*

$$\sigma = \sigma_0 \text{ on } D \subset \partial\Omega. \quad (4.2)$$

- *The conductivity is isotropic or semi-anisotropic so that we assign conductivity to network edge, i.e.,*

$$\sigma(\mathbf{x}) = \text{entry of } \begin{bmatrix} a & 0 \\ 0 & a \end{bmatrix} \text{ or } \begin{bmatrix} a & 0 \\ 0 & b \end{bmatrix}, \text{ not } \begin{bmatrix} a & b \\ b & c \end{bmatrix} \quad (4.3)$$

In addition, noise is usually modeled either additive noise[18], or multiplicative noise. the former is a global background noise and the latter is proportional to local magnitude of current. This paper contains result testing only stability to multiplicative noise. The noise model in this paper is following.

$$\mathbf{J}^\varepsilon(\mathbf{x}) = (1 + \varepsilon \mathbf{R}(\mathbf{x}))\mathbf{J}(\mathbf{x}), \quad (4.4)$$

where $\mathbf{R}(\mathbf{x})$ is a random noise made by a uniform random number generator which produces values between -1 and 1 , and $\varepsilon > 0$ measures the size of the noise.

The stability of the method also depends on the a-priori estimate in (4.1). In the numerical test the true value of each components of the conductivity tensor is between 1 and 5. Since the exact range of the conductivity should not be assumed in the reconstruction process, we assumed that it is between 0.5 and 10. Hence, if a recovered conductivity value is above 10, then it was set as 10. Similarly, any recovered value below 0.5 was set as 0.5 in the recovery process. It is tested in Figure 4.10 that the method becomes unstable as the range of this a-priori estimate increases.

4.2 2D cases

We consider the two dimensional case in this section. If we think of conductivities having a volume at that size of cell h , conductivity in cell is filled with identical values. In isotropic conductivity case, the horizontal and the vertical edge's conductivity are assigned by same value $a_{ij} = b_{ij}$. In semi-anisotropic conductivity case, the horizontal edge is assigned by a_{ij} and the vertical edge by b_{ij} . Finding the resistivity a_{ij} 's and b_{ij} 's from given electrical currents J_{ij}^a 's and J_{ij}^b 's and the boundary resistivity will be called a backward problem in the following. First note that there are $2n(n-1)$ resistors in the system and $4(n-1)$ of them are boundary resistors, which are a_{i0}, a_{in}, b_{0j} and b_{nj} for $1 \leq i, j \leq n-1$. We assume that the resistivity of the boundary material can be observed. In fact, we assume that $2(n-1)$ boundary resistors a_{i0} 's and b_{0j} 's are given and then find the other $2(n-1)^2$ unknown resistors including $2(n-1)$ boundary resistors a_{in} 's and b_{nj} 's. Hence the given boundary region in (4.2) is the one on the x, y -axes, i.e.,

$$\sigma = \sigma_0 \quad \text{on } D \subset \partial\Omega \quad \text{with } D := \{(x, y) : x = 0 \text{ or } y = 0\}. \quad (4.5)$$

Consider a loop given in Figure 4.1, where the currents J_{ij}^a and J_{ij}^b flow along the resistors a_{ij} and b_{ij} , respectively. There are $(n-1)^2$ of such loops and the Kirchhoff's circuit law gives $(n-1)^2$ number of equations:

$$J_{i-1j}^b b_{i-1j} + J_{ij}^a a_{ij} - J_{ij}^b b_{ij} - J_{ij-1}^a a_{ij-1} = 0, \quad 1 \leq i, j \leq n-1. \quad (4.6)$$

Therefore, it is clear that one set of current data is not enough to solve this backward problem and we need at least two sets of current data. However, if an isotropic conductivity is considered, the single set of current data is just enough and we will see that in the following section.

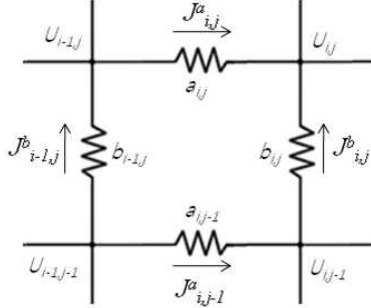


Figure 4.1: A continuous conductivity body is discretized using a resistive network. Then the backward solver is given by the Kirchhoff's voltage (or circuit) law.

There are four unknowns in the equation (4.6). Since the boundary resistivity is assumed to be given, two of them are known if the loop under consideration is the one at the origin. If two sets of the current data are provided, then one can solve (4.6) at the corner loop. One may continue this process until the computation is completed since one can find a loop that two of the resistors are given from previous steps. Note that, if a current vector is given at a grid point (x_i, y_j) , then we may set its x and y components as J_{ij}^a and J_{ij}^b respectively.

4.2.1 2D isotropic conductivity

The conductivity tensor actually gives a scalar multiplication in the isotropic case. For the two dimensional case we may simply set $a_{ij} = b_{ij}$ and consider a_{ij} as this isotropic resistivity at the grid point (x_i, y_j) . Then there are basically n^2 unknowns left since the boundary resistors on the x, y -axes are given. Hence the resistivity can be recovered using a single data set of currents. Suppose that $a_{i-1,j}$ and $a_{i,j-1}$ are given from previous steps. Then a_{ij} is obtained by

$$a_{ij} = \frac{J_{i,j-1}^a}{J_{ij}^a - J_{ij}^b} a_{i,j-1} - \frac{J_{i-1,j}^b}{J_{ij}^a - J_{ij}^b} a_{i-1,j}. \quad (4.7)$$

Note that the setting $a_{ij} = b_{ij}$ for the isotropic case is related to the domain D is given in (4.5). Then, a_{11} can be computed since a_{01} and a_{10} are given. After that, a_{12} and a_{21} can be similarly computed, and one may continue this process increasing $i + j$ as long as $J_{ij}^a - J_{ij}^b \neq 0$.

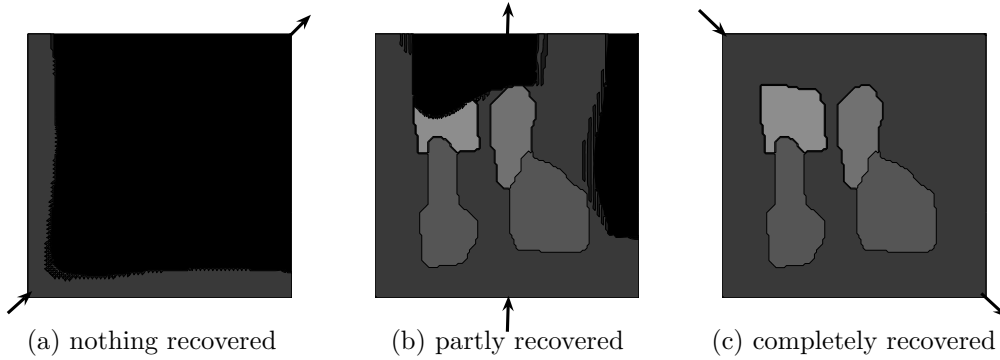


Figure 4.2: Two dimensional isotropic conductivity has been recovered under three different injection currents. Injection currents are denoted by arrows. The best result is (c). In this example noise levels are all zero.

It is clear that if the denominator $J_{ij}^a - J_{ij}^b$ in the reconstruction formula (4.7) is near zero, then the conductivity is not recovered correctly. Hence it is important to consider a injection current to avoid such a situation. First consider the worst the injection current that uses two corner points $(0, 0)$ and $(1, 1)$ (i.e., $g_{00} = g_{nn} = 1$ and all the other boundary currents are zero). Then the main stream of the current is in the direction of vector $(1, 1)$ which will make the denominator in (4.7) be small. In Figure 4.2(a) the results of recovered conductivity is given using this injection current. Even though the numerical computation has been done under very small noise, the conductivity is not recovered at all.

If the current is injected using the points $(0.5, 0)$ and $(0.5, 1)$ as in Figure 4.2(b), some portion of the conductivity is recovered. However, there are spots with poor resolution. It seems that the bad spots start from a point that the electric current becomes parallel to the vector $(1, 1)$. The best case is the one that the current is injected using the points $(1, 0)$ and $(0, 1)$. Then the main stream of the current is aligned to the direction of slope negative one and $J_{ij}^a - J_{ij}^b$ seems to be away from zero. The recovered conductivity is given in Figure 4.2(c) which shows a perfectly recovered image. Note that these images were recovered without noise.

Remark 1. *It was shown that a single set of internal current data is not enough to decide the conductivity image in a unique way (see, e.g., [6, p. 1216]). However, if the conductivity is given on the whole boundary $\partial\Omega$, then such a non-uniqueness examples cannot be constructed. If the boundary conductivity is given partially as in (4.5), then the uniqueness depends on the*

injection currents. If the injection current is given as in Figure 4.2(c), then the examples in [6] do not work since conductivity of the boundary from an injection point to the other one is given and all the equipotential lines are connected to the given boundary. This is another reason for the preferred injection current.

If the injection current in Figure 4.2(a) is employed, then we may consider the model under the assumption that $a_{ij} = b_{i-1j}$ with the given boundary $D := \{(x, y) : x = 1 \text{ or } y = 0\}$. It is also possible to recover the conductivity after dividing the whole domain into several parts. Then, the image of each part of the domain can be computed starting from a corner point and then combined to get the whole picture. For simplicity, we consider the model case $a_{ij} = b_{ij}$ only for the isotropic case and the injecting current given as in Figure 4.2(c) in the following numerical examples.

Remark 2. Notice that under the assumption $a_{ij} = b_{ij}$ for the isotropic case there is a preferred direction of current injection. This non-symmetric structure of the scheme can be removed as following. Let r_{ij} be the resistivity at the grid point (x_i, y_j) . Then, the resistivity a_{ij} and b_{ij} can be replaced as the average of the adjacent resistivity, i.e., (4.6) can be replaced by

$$J_{i-1j}^b \frac{r_{i-1,j} + r_{i-1,j-1}}{2} + J_{ij}^a \frac{r_{ij} + r_{i-1,j}}{2} - J_{ij}^b \frac{r_{ij} + r_{i,j-1}}{2} - J_{ij-1}^a \frac{r_{ij-1} + r_{i-1,j-1}}{2} = 0.$$

Suppose that r_{i-1j}, r_{ij-1} and r_{i-1j-1} are already obtained in the previous steps. Then r_{ij} is obtained by

$$r_{ij} = \frac{J_{ij-1}^a (r_{ij-1} + r_{i-1,j-1}) - J_{i-1j}^b (r_{i-1,j} + r_{i-1,j-1})}{J_{ij}^a - J_{ij}^b} + J_{ij}^b r_{i,j-1} - J_{ij}^a r_{i-1,j}.$$

Hence we still have the same denominator $J_{ij}^a - J_{ij}^b$ and it should be away from zero for the stability. Furthermore the extra addition term $J_{ij}^b r_{i,j-1} - J_{ij}^a r_{i-1,j}$ is another source of noise which is proportional to $(J_{ij}^b - J_{ij}^a)$. Hence this scheme is more sensitive on the noise and the numerical examples show blow-ups even for a low noise level.

It is well known that if the electrical current is perpendicular to the discontinuity of the conductivity image, then such a change is not detectible. In Figure 4.3 such a case is tested and, even with a 25% noise level, the conductivity is recovered reasonably. It is pretty obvious that the boundary conductivity is the source of the information, and it makes the problem stable.

In Figure 4.4, a numerical example using a CT image of a human body as an original conductivity is given. It is possible that certain geometric structure of the body may trigger

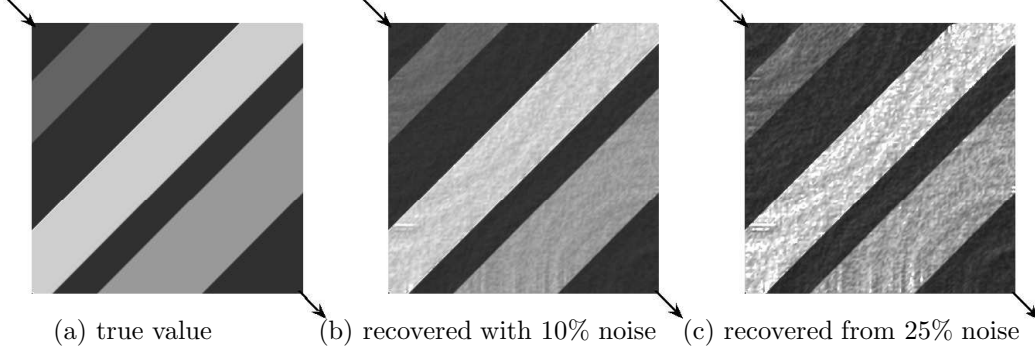


Figure 4.3: This is an example that the discontinuity of the conductivity is orthogonal to the main stream of the current. Since the boundary conductivity is assumed to be given, the conductivity is reasonably recovered even with 25% of noise.

a singularity property of the method. In this example one may observe that even if the noise level is of 25% the two dimensional conductivity is recovered reasonably. However, one may observe a singularity with a noise level higher than this level, which is similar to the third figure in the second row of Figure 4.8.

4.2.2 2D semi-anisotropic conductivity

If the conductivity tensor is a diagonal matrix, which is called a semi-anisotropic case in this paper, the diagonal elements correspond to a_{ij} and b_{ij} for the two dimensional case. If the diagonal entries are positive numbers, then the tensor is positive definite. Hence, we may take any two images to assign the resistivity of vertical and horizontal resistors a_{ij} 's and b_{ij} 's. The total number of resistors for the two dimensional resistive network is $2(n-1)^2 + 2(n-1)$. If $2(n-1)$ boundary resistors a_{i0} 's and b_{0j} 's are given, then $2(n-1)^2$ unknown resistors are left. Since the Kirchhoff's circuit law gives $(n-1)^2$ number of equations in (4.6), it is clear that one set of current data is not enough for the solvability. We should take at least two sets of current data and we denote them by J_{ij}^{ka} and J_{ij}^{kb} , $k = 1, 2$. Then we obtain $2(n-1)^2$ equations:

$$\begin{aligned} J_{ij}^{1a} a_{ij} - J_{ij}^{1b} b_{ij} &= J_{ij-1}^{1a} a_{ij-1} - J_{i-1j}^{1b} b_{i-1j}, \\ J_{ij}^{2a} a_{ij} - J_{ij}^{2b} b_{ij} &= J_{ij-1}^{2a} a_{ij-1} - J_{i-1j}^{2b} b_{i-1j}, \end{aligned} \quad 1 \leq i, j \leq n-1. \quad (4.8)$$

Suppose that a_{ij-1} and b_{i-1j} are boundary resistors or obtained from previous steps. Then a_{ij} and b_{ij} can be computed by solving the 2 by 2 system in (4.8). Therefore, the

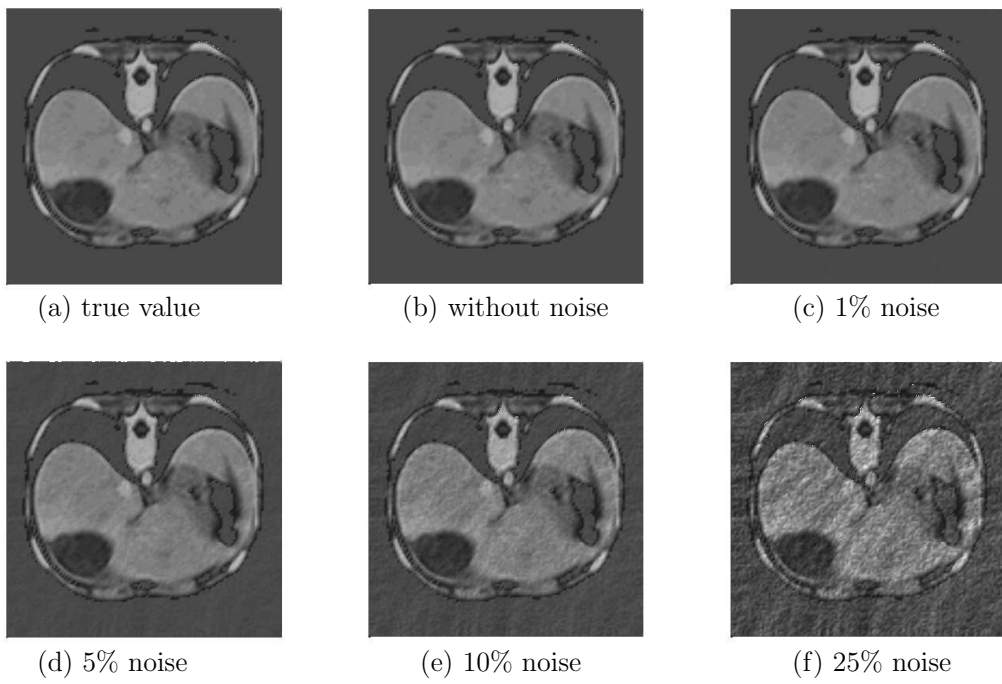


Figure 4.4: Isotropic conductivity recovery in two dimensional space. The noise level is increased up to 25%.

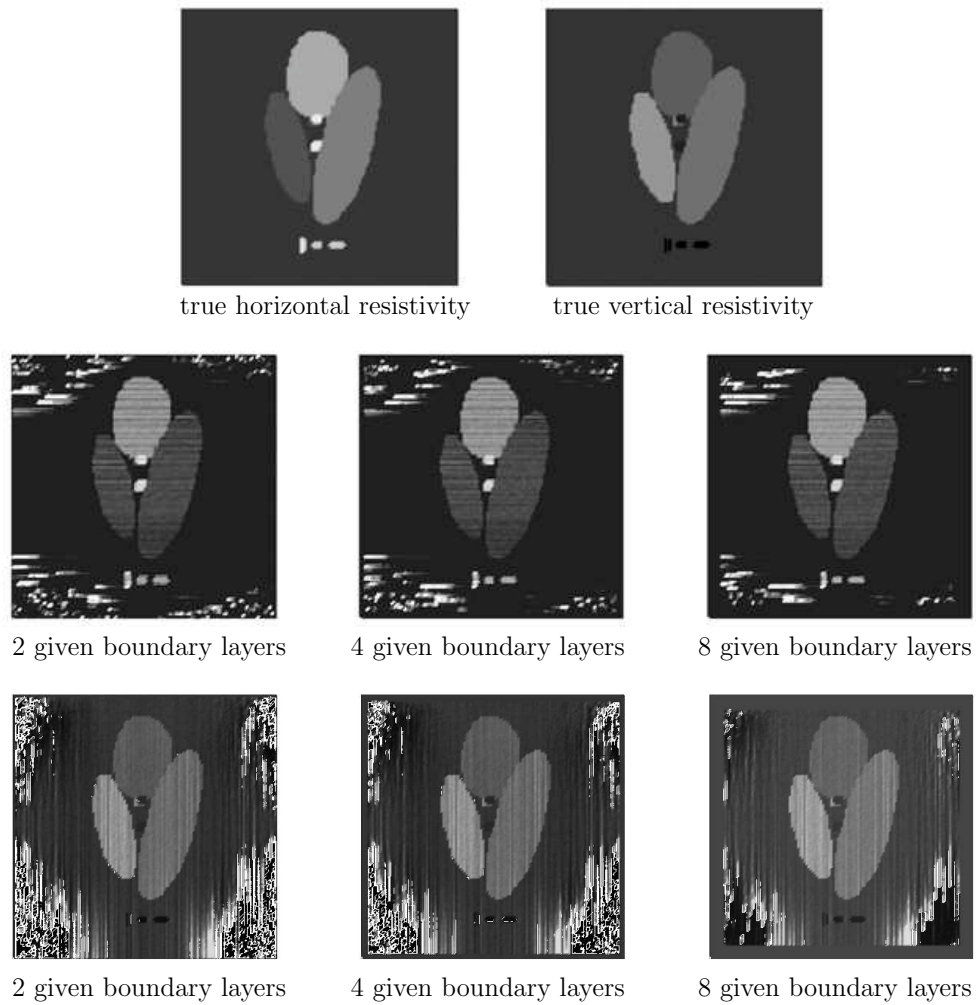


Figure 4.5: Two dimensional semi-isotropic conductivity images obtained as increasing the number of given boundary layers from 2 to 8. The noise level is 5%. The images in the second row are of horizontal resistors a_{ij} 's and the ones in the third row are for b_{ij} 's.

stability of the method depends on the condition number of the matrix

$$A = \begin{pmatrix} J_{ij}^{1a} & J_{ij}^{1b} \\ J_{ij}^{2a} & J_{ij}^{2b} \end{pmatrix}. \quad (4.9)$$

It was observed that there is a preferred direction of injection current for the isotropic case. For the semi-anisotropic case the two sets of current data required in the algorithm have no preferred direction. Note that the isotropic setting $a_{ij} = b_{ij}$ is not used anymore. However, if the two currents \mathbf{J}^1 and \mathbf{J}^2 are parallel at a point, the matrix A becomes singular. Hence, it is important to choose two currents in a way that they make large angles to each other. In the following we compare two approaches.

First, notice that the electrical current becomes parallel to the boundary if the boundary point is away from the boundary current sources. This makes the matrix in (4.9) have a large condition number along the boundary. To reduce this boundary effect the resistors in several boundary layers are assumed to be given. It is tested as increasing the number of given layers in Figure 4.5. The recovered conductivity images show interesting behavior. The conductivity image near the boundary is very poor, which was expected due to the large condition number of the matrix A near boundary. Since the reconstruction technique is performed from the boundary cells, the interior image is expected to show poor resolution from the effect of the poor boundary image. However, the inside image is a lot better than the boundary one. It seems that there is a mechanism that neutralizes the boundary blow-ups. Another interesting thing is that the images of horizontal resistors a_{ij} in the second row of Figure 4.5 show horizontal strips and the images for b_{ij} 's show vertical strips. One may also find similar phenomenon in the three dimensional computations, Figures 4.9 and 4.10 even though the trips are weaker in the three dimensional examples. It seems that this behavior indicates that the noises in the vertical and the horizontal resistors propagate independently. Having the conductivity of several boundary layers is a strong hypothesis. However, even if several boundary layers are assumed to be given, it only makes a small improvement.

The second approach is to increase the number of input nodes. So far we have used only two nodes, which is an extreme case. Now we increase the number of nodes up to forty of them. Note that one of the main advantages of using a resistive network method is that the input current $g(x)$, $x \in \partial\Omega$, is not required in the reconstruction process. Hence one may choose even a random input data using various number of nodes at various places for input currents as long as the condition is satisfied that summation of all boundary injecting current is zero for solvability of neumann problem. This property removes many annoying experimental details that should be considered otherwise. In Figure 4.6 conductivity images

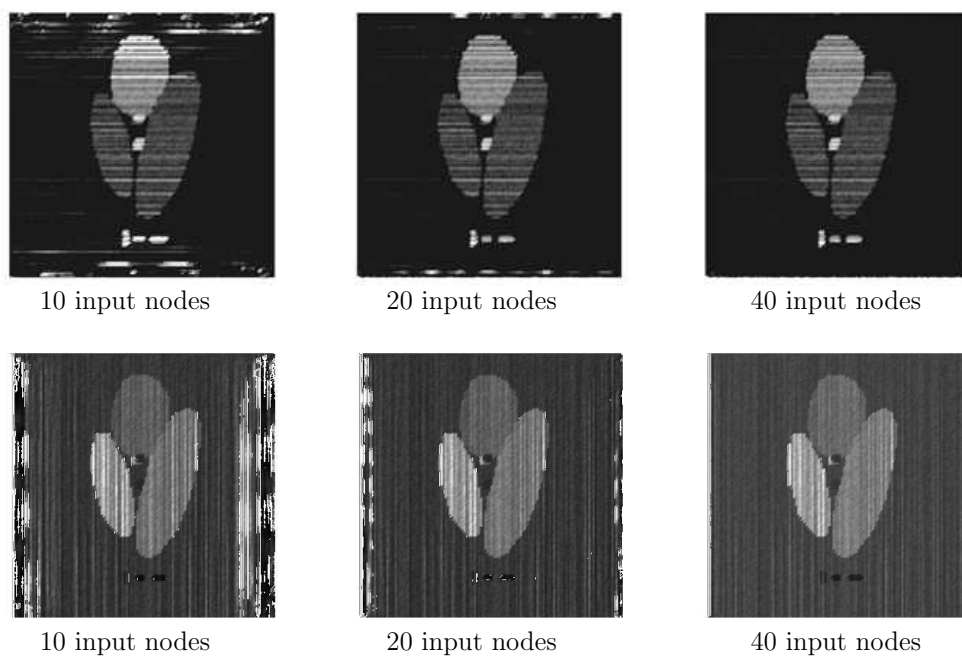


Figure 4.6: Two dimensional semi-isotropic conductivity images obtained as increasing the number of input nodes from 10 to 40. For example, five input nodes were used to each of two parallel sides which totals ten input nodes. The noise level in this example is 10%.

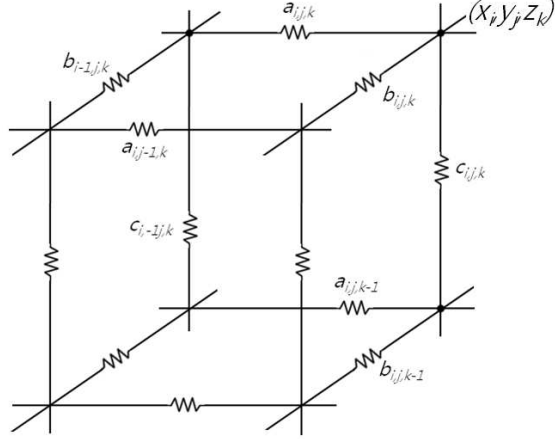


Figure 4.7: A cell of a three dimensional resistive Network

are recovered as increasing the number of input nodes. One may observe that the method becomes more stable as the number of input nodes are increased. This second approach seems the right one to improve the stability of the method.

In these examples one may conclude that the semi-anisotropic case is more unstable in compare with the isotropic one. For the isotropic case the conductivity image has been recovered using only two input nodes with an acceptable resolution even with the noise level 25%. However, the images for the semi-anisotropic case is very poor under the same conditions.

4.3 3D cases

We now consider the three dimensional case. The domain is $\Omega := [0, 1] \times [0, 1] \times [0, 1]$ and the boundary conductivity is assumed to be given on $D \subset \partial\Omega$ given as the following:

$$\sigma = \sigma_0 \text{ on } D \subset \partial\Omega \text{ with } D := \{(x, y) : x = 0, y = 0, \text{ or } z = 0\}. \quad (4.10)$$

A cell for a three dimensional resistive network is given in Figure 4.7. As in the figure, the positive number c_{ijk} denotes the resistor (or its resistivity) below the grid point (x_i, y_j, z_k) . The other resistors a_{ijk} and b_{ijk} are the ones parallel to the x, y -axes, respectively. First note that there are $3n(n-1)^2$ resistors in the system and about $12(n-1)^2$ of them are boundary ones. We assume that boundary resistors on the xy -, xz - and yz -planes, $a_{ij0}, b_{ij0}, a_{i0k}, c_{i0k}, b_{0jk}$ and c_{0jk} 's, are given and then find other $3(n-1)^3$ unknown resistors.

Consider the three faces of the cubic cell in Figure 4.7 that contains the vertex (x_i, y_j, z_k) . If the Kirchhoff's circuit law is applied to each of these three faces, then we obtain

$$\begin{aligned} J_{ijk}^a a_{ijk} - J_{ijk}^b b_{ijk} &= J_{ij-1k}^a a_{ij-1k} - J_{i-1jk}^b b_{i-1jk}, \\ J_{ijk}^b b_{ijk} - J_{ijk}^c c_{ijk} &= J_{ij k-1}^b b_{ij k-1} - J_{ij-1k}^c c_{ij-1k}, \\ J_{ijk}^a a_{ijk} - J_{ijk}^c c_{ijk} &= J_{ij k-1}^a a_{ij k-1} - J_{i-1jk}^c c_{i-1jk}, \end{aligned} \quad 1 \leq i, j, k \leq n-1. \quad (4.11)$$

Suppose that all the resistors are given in previous steps except the ones indexed with ' $_{ijk}$ '. Then the right hand sides are given terms, and the three unknown resistors with subindex ' $_{ijk}$ ' should be computed using these three equations. Adding first two equations gives

$$J_{ijk}^a a_{ijk} - J_{ijk}^c c_{ijk} = J_{ij-1k}^a a_{ij-1k} + J_{ij k-1}^b b_{ij k-1} - J_{ij-1k}^c c_{ij-1k} - J_{i-1jk}^b b_{i-1jk}.$$

Comparing this equation to the third one, one can easily see that the linear system has a solution only if

$$J_{ij-1k}^a a_{ij-1k} - J_{ij k-1}^a a_{ij k-1} + J_{ij k-1}^b b_{ij k-1} - J_{i-1jk}^b b_{i-1jk} - J_{ij-1k}^c c_{ij-1k} - J_{i-1jk}^c c_{i-1jk} = 0.$$

Then, the third equation in (4.11) is the sum of the first two. Hence, we have only two equations applying the Kirchhoff's circuit law to the three dimensional cell. The total number of equations is $2(n-1)^3$, which is enough for the isotropic cases but not for the semi-anisotropic case.

4.3.1 3D Isotropic conductivity

For the three dimensional case we similarly set $a_{ijk} = b_{ijk} = c_{ijk}$ and consider a_{ijk} as the isotropic resistivity value at the grid point (x_i, y_j, z_k) . Then the problem becomes over determined. We rewrite (4.11) as

$$\begin{aligned} a_{ijk} &= (J_{ij-1k}^a a_{ij-1k} - J_{i-1jk}^b a_{i-1jk}) / (J_{ijk}^a - J_{ijk}^b), \\ a_{ijk} &= (J_{i-1jk}^c a_{i-1jk} - J_{ij k-1}^a a_{ij k-1}) / (J_{ijk}^a - J_{ijk}^c), \\ a_{ijk} &= (J_{ij k-1}^b a_{ij k-1} - J_{ij-1k}^c a_{ij-1k}) / (J_{ijk}^b - J_{ijk}^c), \end{aligned} \quad 1 \leq i, j, k \leq n-1. \quad (4.12)$$

Therefore, if $J_{ijk}^a = J_{ijk}^b = J_{ijk}^c$, the problem is unsolvable. If the three terms are close to each other, then the recovery of the conductivity becomes unstable to noises. Hence we need to choose the injection current in a way to avoid such a situation.

The first strategy is to choose one of the three equations that makes the method most stable. Consider three quantities

$$A := \frac{J_{ijk}^a + J_{ijk}^b}{\sqrt{(J_{ijk}^a)^2 + (J_{ijk}^b)^2}}, \quad B := \frac{J_{ijk}^a + J_{ijk}^c}{\sqrt{(J_{ijk}^a)^2 + (J_{ijk}^c)^2}}, \quad C := \frac{J_{ijk}^b + J_{ijk}^c}{\sqrt{(J_{ijk}^b)^2 + (J_{ijk}^c)^2}}.$$

These measure the cosine of the angle between vectors $(1, 1)$ and (J_{ijk}^a, J_{ijk}^b) , (J_{ijk}^a, J_{ijk}^c) or (J_{ijk}^b, J_{ijk}^c) , respectively. Hence we choose the equation corresponding to the smallest one. It seems that this approach is slightly better and solving (4.12) in a least square sense.

The second strategy is to choose an injection current in a way that the main stream of the electric current is orthogonal to the diagonal direction vector $\mathbf{v}_1 := (1, 1, 1)/\sqrt{3}$. For the comparison purpose we consider three kinds of injection currents. We have chosen two points $(0, 0, 0)$ and $(1, 1, 1)$ to apply the first injection current. Then the main current direction is parallel to \mathbf{v}_1 , which should be the worst case. In the first row of Figure 4.8 conductivity images recovered using this current are given. This numerical computation has been done for a three dimensional case with $128 \times 128 \times 128$ mesh and then the slice which is identical to the two dimensional image has been displayed. In this case the image is recovered without noise only. Note that the two dimensional conductivity is not recovered at all even without any noise, Figure 4.2(a). The three dimensional case seems more stable than the two dimensional case.

The second injection current is given through two vertex points $(1, 0, 1)$ and $(0, 1, 0)$. Let $\mathbf{v}_2 := (1, -1, 1)/\sqrt{3}$ be the unit vector that connects these two points. The angle θ between the vectors \mathbf{v}_1 and \mathbf{v}_2 satisfies

$$\cos \theta = \mathbf{v}_1 \cdot \mathbf{v}_2 = 1/3,$$

i.e., the angle $\theta \cong 70.5$ in degree. In the second row of Figure 4.8 conductivity images recovered using this current are given. In this case the conductivity is well recovered even with high noise levels. In compare with Figure 4.2(b) this three dimensional case is more stable than the two dimensional case. Note that, under the noise level of 40%, there is a black strip in the middle of the left half.

The last injection current uses two middle points of edges, $(0, 1, 0.5)$ and $(1, 0, 0.5)$. Let $\mathbf{v}_3 := (1, -1, 0)/\sqrt{2}$ be the unit vector that connects these two points. This vector is orthogonal to the diagonal direction, i.e.,

$$\cos \theta = \mathbf{v}_1 \cdot \mathbf{v}_3 = 0.$$

In the third row of Figure 4.8 three images recovered using this injection current are given. The recovered images are better than the ones in the second row. In particular the one of noise level of 40% does not have a black strip in this case.

4.3.2 3D semi-anisotropic case

It is clear that a single set of current data is not enough to decide the semi-anisotropic conductivity and hence we use two sets of current data for the backward solver. Let \mathbf{J}^1 and

\mathbf{J}^2 be two given currents. Then the Kirchhoff's circuit law gives four equations for each cell:

$$\begin{aligned}
J_{ijk}^{1a} a_{ijk} - J_{ijk}^{1b} b_{ijk} &= J_{i,j-1,k}^{1a} a_{i,j-1,k} - J_{i-1,j,k}^{1b} b_{i-1,j,k}, \\
J_{ijk}^{1b} b_{ijk} - J_{ijk}^{1c} c_{ijk} &= J_{i,j,k-1}^{1b} b_{i,j,k-1} - J_{i,j-1,k}^{1c} c_{i,j-1,k}, \\
J_{ijk}^{2a} a_{ijk} - J_{ijk}^{2b} b_{ijk} &= J_{i,j-1,k}^{2a} a_{i,j-1,k} - J_{i-1,j,k}^{2b} b_{i-1,j,k}, \\
J_{ijk}^{2b} b_{ijk} - J_{ijk}^{2c} c_{ijk} &= J_{i,j,k-1}^{2b} b_{i,j,k-1} - J_{i,j-1,k}^{2c} c_{i,j-1,k},
\end{aligned} \quad 1 \leq i, j, k \leq n-1. \quad (4.13)$$

In Figure 4.9 a numerical example for three dimensional semi-anisotropic conductivity reconstruction is given. First, for this experiment, a three dimensional cubic domain $\Omega = [0, 1]^3$ is discretized into 128^3 cubic cells and three dimensional images have been constructed for resistors a_{ijk} 's, b_{ijk} 's, and c_{ijk} 's. For the current injections, two kinds of injection currents are applied using 20 input nodes. The first set of electrical current data is measured after applying the boundary current on two sides which are parallel to the yz -plan. The second one is measured after applying the currents on the sides parallel to xz -plan. Note that these two currents are mostly move to the direction of x and y axes. Hence z -component of the current is weaker than others.

The images for a_{ijk} 's and b_{ijk} 's in Figure 4.9 are in a good shape. However, the one for c_{ijk} 's is poor. It needs to make the current move to the direction of z -axis or add this current to use three sets of data to obtain a better conductivity image related to that direction. The images for a_{ijk} 's and b_{ijk} 's are in a good shape even with 25% noise. There are lines in the images which is weaker than the ones of the two dimensional cases. One can clearly observe that this three dimensional case is more stable than the two dimensional one.

In this example each component of the true conductivity is between 1 and 5. In the construction process, it is assumed that we have an a-priori estimate that conductivity satisfies $0.5 \leq \sigma \leq 10$. Hence any reconstructed conductivity value higher than 10 was set as 10. Similarly, any value below 0.5 was set as 0.5. In Figure 4.10, the performance is tested under different a-priori estimates. The first row of the figure is simply a different slice of the previous example which uses the same a-priori estimate $0.5 \leq \sigma \leq 10$. The images in the second and third rows were built using a-priori estimates $0.25 \leq \sigma \leq 20$ and $0.125 \leq \sigma \leq 40$, respectively. In the figures one can clearly observe that the performance of the method strongly depends on the a-priori estimate of the conductivity. Since recovering process takes only couple of minutes, we may vary these a-priori estimates after seeing the results on treatment time, though.

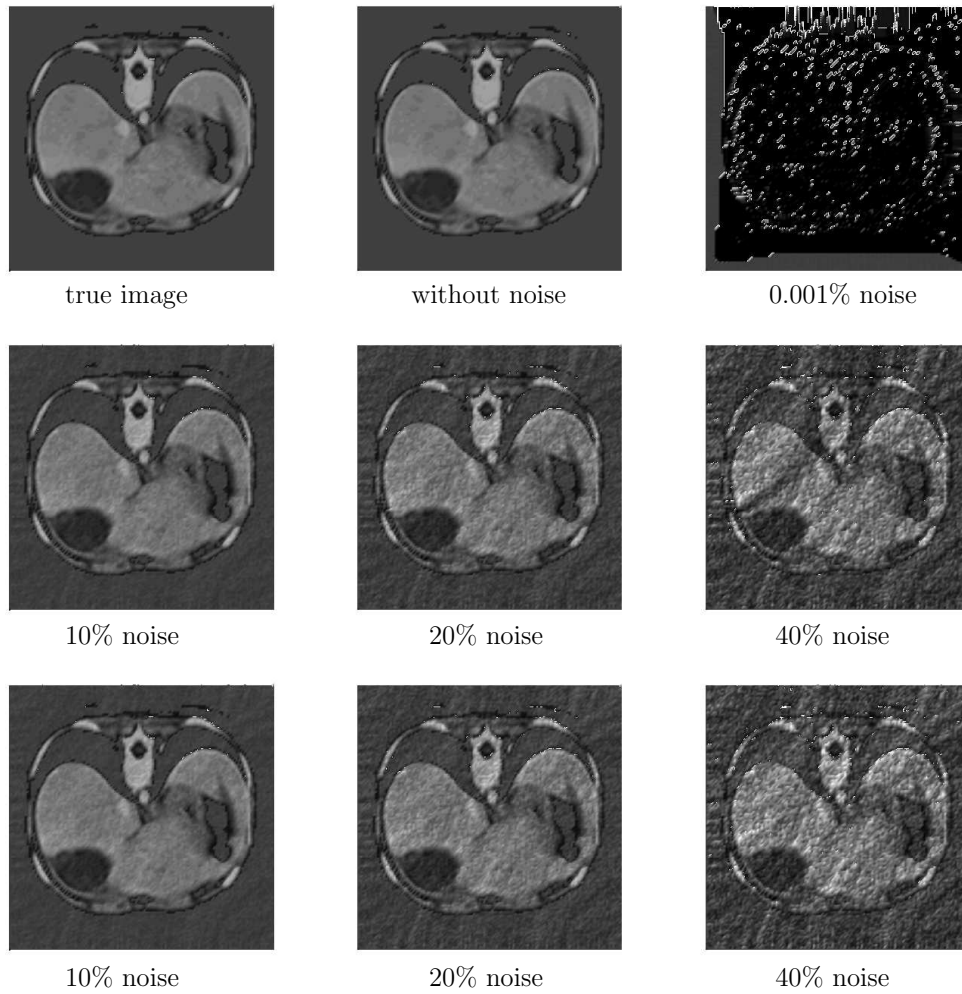


Figure 4.8: Isotropic conductivity image in three dimension. Injection current for the first row is given through two points $(0, 0, 0)$ and $(1, 1, 1)$. The second row uses $(1, 0, 1)$ and $(0, 1, 0)$ and the third one uses $(0, 1, 0.5)$ and $(1, 0, 0.5)$.

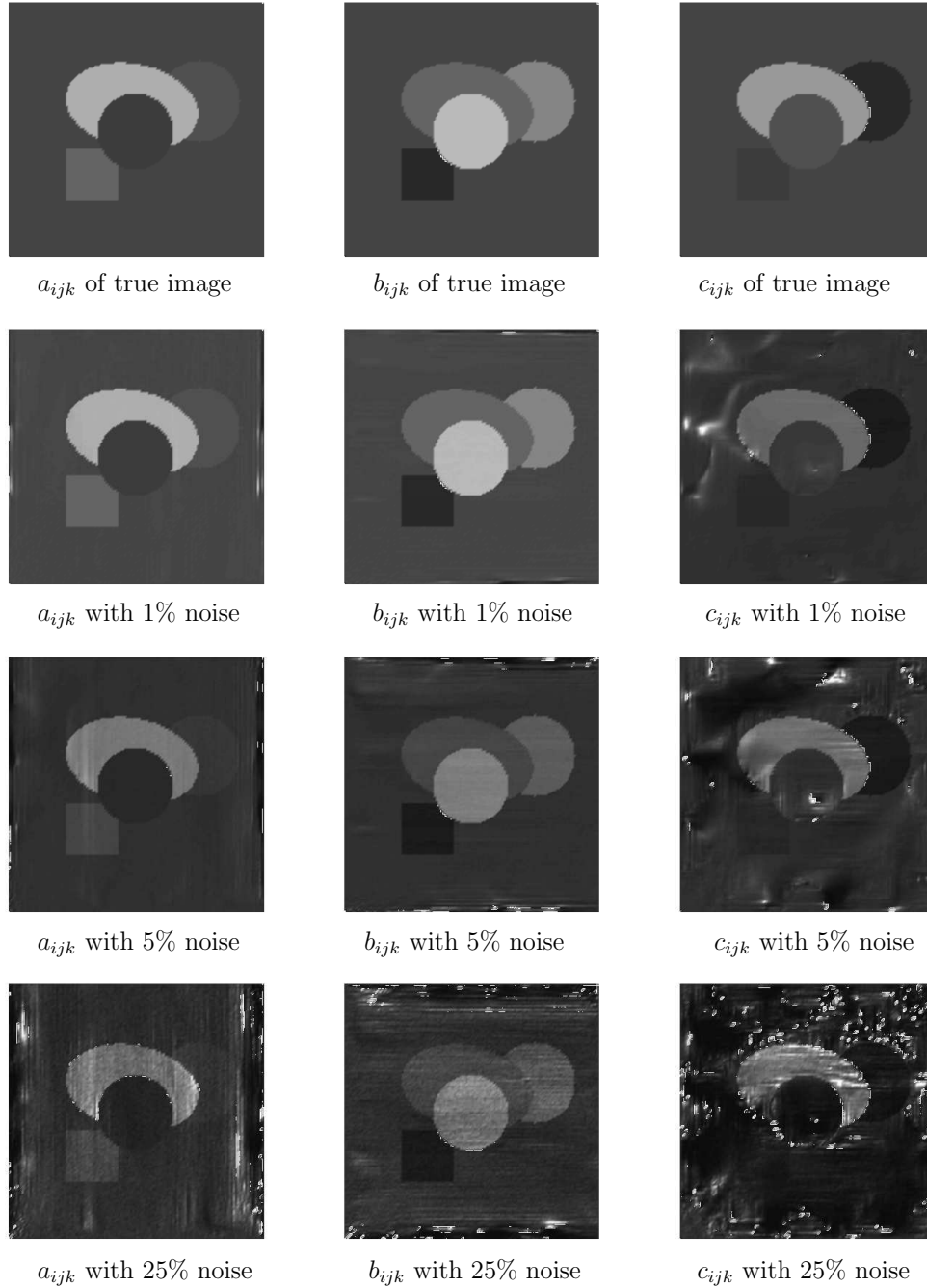
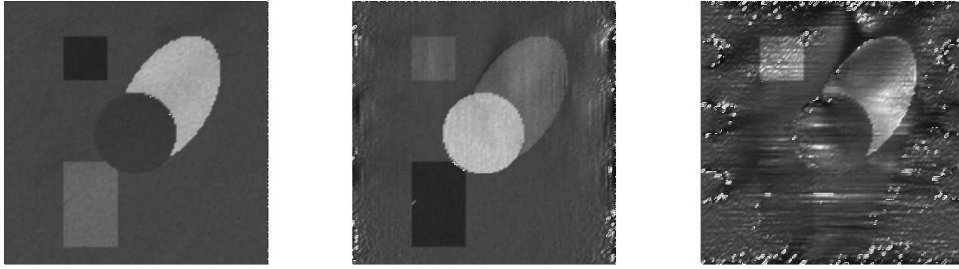
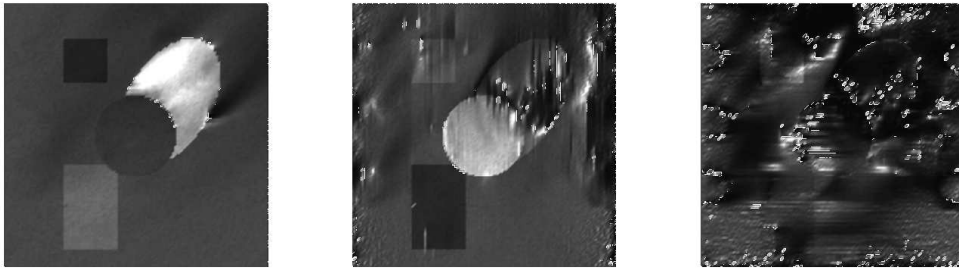


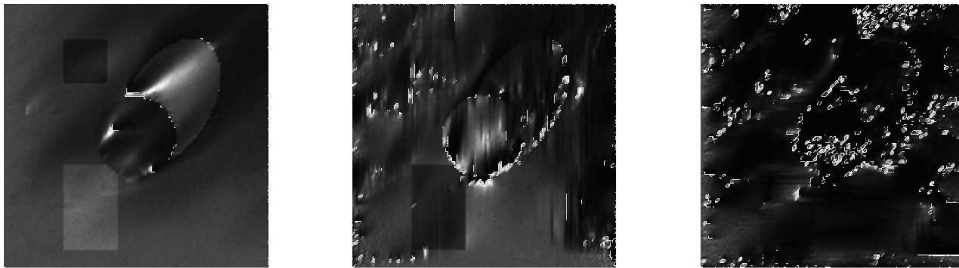
Figure 4.9: Three dimensional semi-anisotropic conductivity images. Two sets of injection currents are applied in the direction of x and y -axes. These figures are slices of three dimensional body orthogonal to the z -axis with $k = 68$ out of 128. The image for c_{ijk} is worse than others since the current in the direction is weaker.



Images for a_{ijk} , b_{ijk} and c_{ijk} reconstructed under a-priori estimate: $0.5 \leq \sigma \leq 10$.



Images for a_{ijk} , b_{ijk} and c_{ijk} reconstructed under a-priori estimate: $0.25 \leq \sigma \leq 20$.



Images for a_{ijk} , b_{ijk} and c_{ijk} reconstructed under a-priori estimate: $0.125 \leq \sigma \leq 40$.

Figure 4.10: Three dimensional semi-anisotropic conductivity images. Two sets of injection currents are applied in the direction of x and y -axes. These figures are slices of three dimensional body orthogonal to the x -axis with $i = 60$ out of 128 layers. The actual conductivity is range is $1 \leq \sigma \leq 5$. The noise level of this example is 10%.

5. Conclusions

When a non-iterative MREIT method for a static conductivity image is applicable is discussed in chapter 3 and has been developed on a resistive network in chapter 4. The image for an isotropic case is reconstructed from a single set of internal current and the boundary conductivity. Two sets of current data are used for a semi-anisotropic case that the conductivity tensor is given as a diagonal matrix. The numerical stability tests for various cases have been performed. For the test a multiplicative random noise has been added to the current and the conductivity has been reconstructed using this noised data. The recovered images indicate that the method has certain stability property. Three dimensional examples show more stable behaviors than the two dimensional ones. The noise level can be increased up to 40% for three dimensional isotropic case. For the three dimensional semi-anisotropic case is done with up to 25% noise level. Since this is a direct method based on the Kirchhoff's laws of current and voltage, the computation time is minimum. It only takes couple of minutes for the three dimensional computation with 128^3 meshes on a personal computer. So one may try various configuration on the same data considering one's own target rather than try to set conditions once. Unfortunately, the rectangular network in this paper is not general enough to handle the fully anisotropic case because we can't know the each direction of eigenvectors of anisotropic tensor. It seems that a network with a flexible structure is required to handle the case if there is one. Obtaining one will be a real challenge in the future. Another thing that should be considered is a denoising technique that fits to the proposed method. We only tested how the method works under noise. We expect that a proper denoising technique may improve the performance. In addition, since other researchers frequently use additive noise model which is based on the paper Scott[18], to test stability about this noise model is still remained task to do. Also, If we implement B_z -based network approach before we investigate anisotropic case, we can experience phenomenon to handle the situation more degrees of freedom are added.

6. Appendix : Stability analysis

In this section we will see that a classical stability analysis of a linear system shows the stability of the conductivity reconstruction method discussed in this paper. For simplicity, we consider a two dimensional semi-anisotropic conductivity in the following discussion. The total number of resistors for such a case is $2n^2 + 2n$. The $2n$ boundary resistors, a_{i0} 's and b_{0j} 's, are assumed to be given. Hence the total number of unknown resistors is $2n^2$. If the currents J_{ij}^a and J_{ij}^b that flow through the resistors a_{ij} and b_{ij} , respectively, are given for $0 \leq i, j \leq n-1$, then the Kirchoff's circuit law gives n^2 number of equations as in (4.6). In the numerical examples two or more sets of current data can be used. In doing that two equations has been chosen in the way that the corresponding 2×2 matrix has the smallest condition number among other possible choices.

In the followings we consider the currents which are chosen in a way that the following matrix

$$A = \begin{pmatrix} J_{ij}^{1a} & J_{ij}^{1b} \\ J_{ij}^{2a} & J_{ij}^{2b} \end{pmatrix}$$

is not singular. Then we solve the following $2n^2$ equations:

$$\begin{aligned} J_{ij}^{1a}a_{ij} - J_{ij}^{1b}b_{ij} + J_{i-1j}^{1b}b_{i-1j} - J_{ij-1}^{1a}a_{ij-1} &= 0, \\ J_{ij}^{2a}a_{ij} - J_{ij}^{2b}b_{ij} + J_{i-1j}^{2b}b_{i-1j} - J_{ij-1}^{2a}a_{ij-1} &= 0, \end{aligned} \quad 1 \leq i, j \leq n-1. \quad (6.1)$$

Since a_{i0} 's and b_{0j} 's are given, these $2n^2$ equations can be written as

$$C\mathbf{y} = \mathbf{f}, \quad (6.2)$$

where $C = (c_{ij})$ is a $2n^2 \times 2n^2$ sparse matrix consists of the coefficients J_{ij}^{1a} , J_{ij}^{1b} , J_{ij}^{2a} and J_{ij}^{2b} and the vector \mathbf{y} is $2n^2$ column vector consists of $2n^2$ unknown resistors. The right hand side column vector \mathbf{f} appears due to the given boundary resistors and hence it has at most $2n-1$ nonzero elements.

For the stability analysis consider perturbed current data $\tilde{\mathbf{J}}_{ij}^k$'s with $k = 1, 2$. Then the actual linear system one may obtain is an approximation of (6.2) that is written as

$$\tilde{C}\tilde{\mathbf{y}} = \tilde{\mathbf{f}}. \quad (6.3)$$

Now we test the stability of the problem. Let

$$\mathbf{e} = \tilde{\mathbf{y}} - \mathbf{y}, \quad E = \tilde{C} - C, \quad \mathbf{h} = \tilde{\mathbf{f}} - \mathbf{f} \quad \text{and} \quad \mathbf{H}_{ij}^k = \tilde{\mathbf{J}}_{ij}^k - \mathbf{J}_{ij}^k, \quad 0 \leq i, j \leq n-1, \quad k = 1, 2.$$

The condition number of a nonsingular matrix C is $\kappa = \text{cond}(C) := \|C\|_\infty \|C^{-1}\|_\infty$. First we consider the solvability of the perturbed problem which depends on the following lemma:

Lemma 1 (Neumann Lemma). *If $\|C^{-1}\|_\infty \cdot \|E\|_\infty < 1$, then $I + C^{-1}E$ is invertible. Hence $C(I + C^{-1}E) = C + E = \tilde{C}$ is invertible, too.*

One can easily see that $E = \tilde{C} - C$ has at most four nonzero elements in each row. Hence, it is clear that

$$\begin{aligned} \|E\|_\infty &= \max_{1 \leq i \leq 2(n-1)^2} \left(\sum_{j=1}^{2n^2} |e_{ij}| \right) \leq 4 \max_{0 \leq i, j \leq (n-1)} (|H_{ij}^{1a}|, |H_{ij}^{1b}|, |H_{ij}^{2a}|, |H_{ij}^{2b}|), \\ \|\mathbf{h}\|_\infty &= \max_{1 \leq i \leq 2(n-1)^2} |h_i| \leq \max_{0 \leq i, j \leq (n-1)} (|a_{i0} H_{i0}^{1a}|, |b_{0j} H_{0j}^{1b}|, |a_{i0} H_{i0}^{2a}|, |b_{0j} H_{0j}^{2b}|). \end{aligned} \quad (6.4)$$

Therefore, if

$$\max_{0 \leq i, j \leq n-1} (|H_{ij}^{1a}|, |H_{ij}^{1b}|, |H_{ij}^{2a}|, |H_{ij}^{2b}|) < \frac{1}{4\|C^{-1}\|_\infty} = \frac{\|C\|_\infty}{4\kappa}, \quad (6.5)$$

the perturbed problem (6.3) is solvable. Using (6.2) the perturbed system can be written as

$$(C + E)\mathbf{e} = \mathbf{h} - E\mathbf{y},$$

and

$$\mathbf{e} = (C + E)^{-1}(\mathbf{h} - E\mathbf{y}) = (I + C^{-1}E)^{-1}C^{-1}(\mathbf{h} - E\mathbf{y}).$$

Hence the error $\mathbf{e} = \tilde{\mathbf{y}} - \mathbf{y}$ is estimated by

$$\|\mathbf{e}\|_\infty \leq \frac{\|C^{-1}\|_\infty}{1 - \|C^{-1}E\|_\infty} (\|\mathbf{h}\|_\infty + \|E\|_\infty \|\mathbf{y}\|_\infty).$$

Since the exact solution \mathbf{y} is bounded by the maximum resistivity, and E and \mathbf{h} are bounded by (6.4), the error is estimated by

$$\|\mathbf{e}\|_\infty \leq \frac{\|C^{-1}\|_\infty}{1 - \|C^{-1}E\|_\infty} [5R \max_{0 \leq i, j \leq n-1} (|H_{ij}^{1a}|, |H_{ij}^{1b}|, |H_{ij}^{2a}|, |H_{ij}^{2b}|)], \quad (6.6)$$

where R is the maximum resistivity. Hence the error \mathbf{e} decays to zero as the noise of the current data converge to zero. Therefore, under the stability condition (6.5), the approximation error of the method is uniformly bounded by (6.6).

요약문

네트워크 모델을 통한 전도도의 복구

MREIT에서 역문제란 다음의 전기적 관계를 이용하여, 인체 내부의 전도도를 복구하려는 것이다.

$$\begin{cases} -\nabla \cdot (\sigma \nabla u) = 0 & \text{in } \Omega \\ -\sigma \nabla u = g & \text{on } \partial\Omega \end{cases}$$

$u(\mathbf{x})$ 는 포텐셜, $\sigma(\mathbf{x})$ 전도도, 그리고 $-\sigma \nabla u (= \mathbf{J})$ 는 전류밀도이다. \mathbf{J} 또는 자기장 \mathbf{B} 이 주어졌을 때, 내부의 전도도 $\sigma(\mathbf{x})$ 를 알고자 한다.

이러한 종류의 식은 다양한 분야의 모델에서 풍부하게 나타난다. 평형상태와 확산현상을 표현하는 식이다. 따라서 위의 역문제를 푸는 것은 전기적 관계에서 전도도문제만을 푸는 것이 아닐 것이다. 이러한 관점에서, 위의 현상을 네트워크 모델로써 근사하려는 것은 전혀 새로운 접근은 아니다.[21] 역학에서의 힘의 평형, 앞서의 전기적 관계 등에서 볼 수 있다. 따라서 우리는 자연스럽게 네트워크 모델을 도입하며, 이것은 연속영역에서 주어지는 미분방정식의 차분법 또는 적분폼으로서 그 근거를 찾을 수 있다. 네트워크 모델은 그동안 많은 MREIT 연구자들이 다루어 온 \mathbf{J} , B_z , σ 사이의 관계를 선형모델로서 설명해준다.

첫번째 장에서는 MREIT 문제를 소개하고, 2장에서는 1992년 이래의 연구가 진행되어 온 과정을 살펴본다. 3장에서는 네트워크 모델이 그동안의 연구와 어떤 관계에 있는지를 설명해보고 이의 선형화된 설명을 시도해 본다. 그리고 4장에서는 네트워크 접근법을 시뮬레이션한 결과를 보고하며, 이 방법이 노이즈에 대해 안정성이 있고, 빠르게 풀리는 방법임을 보고한다.

References

- [1] Birgul O, Ider Y Z, 1995, Use of the magnetic field generated by the internal distribution of injected currents for electrical impedance tomography, *Proc. 9th Int. Conf. Elec. Bio-Impedance (Heidelberg, Germany)* pp 418 9
- [2] Birgul O and Ider Y Z, 1996, Electrical impedance tomography using the magnetic field generated by injected currents, *Proc. 18th Ann. Int. Conf. IEEE EMBS (Amsterdam, Netherlands)* pp 784 5
- [3] Ider Y Z and Birgul O, 1998, Use of the magnetic field generated by the internal distribution of injected currents for electrical impedance tomography, *Elektrik* **6** 215 25
- [4] Ider Y Z, Onart S and Lionheart W R B, 2003, Uniqueness and reconstruction in magnetic resonance electrical impedance tomography (MREIT), *Physiol. Meas.* **24** 591 604
- [5] Ider Y Z and Onart S, 2004, Algebraic reconstruction for 3D MREIT using one component of magnetic flux density, *Physiol. Meas.* **25** 281 94s
- [6] Kim Y J, Kwon O, Seo J K and Woo E J 2003 Uniqueness and convergence of conductivity image reconstruction in magnetic resonance electrical impedance tomography, *Inverse Problems* **19** 1213 25
- [7] Kwon O, Woo E J, Yoon J R and Seo J K, 2002, Magnetic resonance electrical impedance tomography (MREIT): simulation study of J -substitution algorithm, *IEEE Trans. Biomed. Eng.* **48** 160 7
- [8] Kwon O, Lee J Y and Yoon J R, 2002, Equipotential line method for magnetic resonance electrical impedance tomography (MREIT), *Inverse Problems* **18** 1089 100
- [9] Kwon O, Park C, Park E J, Seo J K and Woo E J, 2005, Electrical conductivity imaging using a variational method in B_z -based MREIT *Inverse Problems* **21** 969 80
- [10] Kwon O, Pyo H, Seo J K and Woo E J, 2006, Mathematical framework for B_z -based MREIT model in electrical impedance imaging, *Int. J. Comput. Math. Appl.* **51** 817 28
- [11] Lee B I, Oh S H, Woo E J, Lee S Y, Cho M H, Kwon O, Seo J K, Lee J Y and Baek W S, 2003b, Three-dimensional forward solver and its performance analysis in magnetic

- resonance electrical impedance tomography (MREIT) using recessed electrodes, *Phys. Med. Biol.* **48** 1971 86
- [12] Nachman A, Tamasan A and Timonov A, 2007, Conductivity imaging with a single measurement of boundary and interior data, *Inverse Problems* **23** 2551 63
- [13] Nam H S, Park C, Kwon O, 2008, Non-iterative conductivity reconstruction algorithm using projected current density in MREIT, *Phys. Med. Biol.* **53**
- [14] Oh S H, Lee B I, Woo E J, Lee S Y, Cho M H, Kwon O and Seo J K, 2003b, Conductivity and current density image reconstruction using harmonic B_z algorithm in magnetic resonance electrical impedance tomography, *Phys. Med. Biol.* **48** 3101 16
- [15] Park C, Kwon O, Woo E J and Seo J K, 2004, Electrical conductivity imaging using gradient B_z decomposition algorithm in magnetic resonance electrical impedance tomography (MREIT), *IEEE Trans. Med. Imaging* **23** 388 94
- [16] Park C, Park E J, Woo E J, Kwon O and Seo J K, 2004, Static conductivity imaging using variational gradient B_z algorithm in magnetic resonance electrical impedance tomography, *Physiol. Meas.* **25** 275 69
- [17] Park C, Lee B I, Kwon O, 2007, Analysis of recoverable current from one component of magnetic flux density in MREIT and MRCDI, *Phys. Med. Biol.* **52**
- [18] Scott G C, Joy M L G, Armstrong R L and Hankelman R M, 1992, Sensitivity of magnetic resonance current density imaging *J. Magn. Reson.* **97** 235 54
- [19] Seo J K, Yoon J R, Woo E J, Kwon O, 2003, Reconstruction of conductivity and current density Images using only one component of magnetic field measurements, *IEEE Trans. Biomed. Eng* **50**
- [20] Seo J K, Kwon O, Lee B I, Woo E J , 2003, Reconstruction of current density distributions in axially symmetric cylindrical sections using one component of magnetic flux density: computer simulation study, *Physiol. Meas.* **24**
- [21] Gilbert Strang, 1986, Introduction to Applied Mathematics, *Wellesley-Cambridge Press* pp.
- [22] Woo E J, Lee S Y and Mun C W, 1994, Impedance tomography using internal current density distribution measured by nuclear magnetic resonance *Proc. SPIE* **2299** 377 85

- [23] Woo E J, Seo J K, 2008, Magnetic resonance electrical impedance tomography(MREIT) for high-resolution conductivity imaging, *Physiol. Meas.* **29** R1-R26
- [24] Zhang N, 1992, Electrical impedance tomography based on current density imaging *MS Thesis* University of Toronto, Toronto, Canada

감사의 글

이 논문을 완성하기까지 주위의 모든 분들로부터 수많은 도움을 받았습니다.

먼저 저를 낳아주시고 길러주신 부모님께 감사드립니다. 부모님으로부터 어떤 것을 대하는 긍정적이고 편안한 태도를 배웠습니다. 그리고 언제나 생각하면 든든함을 주는 형이 있어서 저도 더 자유롭게 살고 있습니다. 그리고 사랑하는 아내 선경이에게 고마움은 이루 말할 수 없습니다. 비록 저의 짧은 학위논문이었지만, 쓰는 내내 옆에 있어준 것이 고맙고, 이렇게 함께 삶을 꾸리며 살고 있는 것이 고맙습니다. 아직 이렇게 감사인사 외에 많이 해드릴 수 없는데도, 늘 막내아들처럼 사위를 맞아주시는 친부모님과 다를 바 없으신 장인어른, 장모님께도 감사드립니다. 또 정말 친동생처럼 아껴주는 민경누나, 종태형도 고맙습니다.

지도교수님이 계셔서 학부연구프로그램으로 들어와 석사2년이 지나는 동안 안심하고 공부하며 이렇게 한차례 석사학위 졸업을 맞고 공부하게 되었습니다. 혹 설픈 생각을 해도 인내심으로 기다려주셔서 그럴 수 있었습니다. 학생의 이야기를 파트너처럼 진지하게 들어주시고 토론하곤 해서 저도 신나게 말하고 연구했던 것 같습니다. 학부때 학과장님으로써, 지금은 지나칠때마다 염려와 조언의 말씀을 가끔 해주셨던 김홍오 교수님, 학부지도 교수님이지만 열정으로 아직도 제게 힘이 되어주시는 이창욱교수님께 감사드립니다. 처음 저희 연구에 많은 도움과 애정을 주셨던 김혜현 교수님께도 감사드립니다. 저희 학생들을 염려해주시는 저희과 모든 교수님들께 진심으로 감사드립니다.

연구실에서 늘 한편으로 누나같고 한편으로 선배님이셨던 조은주 박사님이 계셔서 큰 힘이 되었습니다. 순수하고 공부에대한 태도로 연구실 분위기의 키를 잡아주는 재환씨, 귀엽고 언제나 주변사람들을 좋은마음으로 대해주는 우리 Eugenia 경림이, 새로 와서도 벌써 큰 힘이 되어주고 있는 성실한 창욱씨, 우리 연구실에 이제 빠져서는 안될 민수씨에게도 감사드립니다. 처음 제게 7-1부터 수치해석 연습을 시켜주셨던 하영수 박사님, 계실때 더 많이 배웠어야 했는데 아쉽지만 큰 누나같던 이영란 교수님, 늘 격의없고 겸손한 태도로 저희 이야기를 들어주시는 이영수박사님, 늘 열심이시고 무슨 말이든 들어주실 거 같은 김정애박사님께도 감사드립니다.

같이 대학원에 들어와서 서로 부족함도 메꿔주고 고민도 나눈 동기들, 선호형, 진혁씨, 진형씨도 어디에 있든 함께하는 마음이었으면 합니다. 저의 삶에 함께해 주었던 친구들, 민호형, 형민이형, 지수, 동현이, 준학이, 기석이, 선경이 친구들 미용이, 덕우형, 영아에게도 저희 가족에게 베푼 따뜻한 마음 감사히 생각합니다.

저의 이 작은 결실이 그분들께 조금이나마 보답이 되기를 바랍니다.

이 력 서

이 름 : 이 민 기

생 년 월 일 : 1981년 9월 2일

출 생 지 : 서울 은평구 응암동

주 소 : 대전 유성구 공동 KAIST아파트 102동 5-1호

E-mail 주 소 : miya@kaist.ac.kr

학 력

1997. 3. - 1999. 2. 한성과학고등학교 (2년 수료)

1999. 3. - 2007. 8. 한국과학기술원 수리과학과 (B.S.)

경 력

2003.12. - 2005.12 국군수송사령부 육군

2008. 3. - 2008. 6. 한국과학기술원 수리과학과 미적조교

2009. 2. - 2009. 5. 한국과학기술원 Freshmen Design 조교

학 회 활 동

1. Yong-Jung Kim, **Min-Gi Lee**, *A direct method for a conductivity recovery using a resistive network*, *KSIAM 2008 Annual Meeting*, November 28~29, 2008, Suanbopark Hotel, Chungju, Korea